

POLITECNICO DI TORINO

Master Degree in Mechanical Engineering

Master's Degree Thesis

**A Deterministic Dynamic
Programming Algorithm for Series
Hybrid Architecture Layout
Optimization**



Academic Supervisor:

Prof. Daniela MISUL

Graduate:

Mattia PERRONE

ACADEMIC YEAR 2018-2019

Abstract

The design of powertrains in hybrid vehicles represents a complex problem due to the many possible components' configuration and sizing. The present work is focused on the implementation of a series hybrid vehicle layout, building upon the *optimization tool* developed in [1]. The tool is aimed at the evaluation of an optimal control strategy of hybrid vehicles by means of a deterministic dynamic programming algorithm. Several layouts can therefore be compared in terms of emissions over a selected driving cycle. Two control methods are proposed and compared. The second differs from the first in that it allows to directly control the internal combustion engine speed. Thus this permits to properly assess for the inertial power of the rotating masses of all powertrain components, which is not achievable with the first control strategy.

Contents

List of Tables	4
List of Figures	5
1 Introduction	7
1.1 Introduction to hybrid vehicles	7
1.2 Classification of hybrid vehicles	8
1.2.1 Series hybrid vehicles	9
1.2.2 Parallel hybrid vehicles	9
1.2.3 Series-parallel hybrid vehicles	10
1.2.4 Electric machines position classification	11
2 Concept and Design of an Optimization Tool for HEVs	13
2.1 Dynamic programming optimization	13
2.1.1 Cost-to-go function	14
2.1.2 Deterministic problems	14
2.1.3 Optimal policy definition	14
2.1.4 Algorithm	15
2.2 Time discretization	16
2.3 Input variables	18
2.4 Control variables	18
2.5 State variables	19
2.6 Configuration matrices approach	20
2.7 Intermediate variables	20
2.8 Optimization phase	22
2.9 Vehicle components	23
2.9.1 Internal combustion engine	23
2.9.2 Electric machine	23
2.9.3 Battery	25
2.9.4 Torque coupling device	27
3 Series architecture implementation	29
3.1 P2P4 layout	31
3.2 Proposed model	32

3.2.1	Evaluation of the requested power	34
3.2.2	Metamap	35
3.3	Control strategies	36
3.3.1	Working-modes control	39
3.3.2	Speeds control	42
4	Results	45
4.1	Comparison between working-modes control and speeds control	46
4.1.1	Considerations on computational time	48
4.2	Power profiles	48
4.3	State of charge and powerflow profiles	50
5	Conclusions	53
	Bibliography	55

List of Tables

2.1	Elementary cell properties	25
3.1	$p2p4$ working modes	33
3.2	Representation of speed variations combinations on a single time interval	43
4.1	Heavy-duty Vehicle Parameters.	45
4.2	Series layout adopted for the comparison between different control strategies.	47

List of Figures

1.1	Parallel Double Shaft hybrid vehicle.	9
1.2	Series-parallel layout.	11
2.1	Discretization of time domain	17
2.2	Electric machine conversion efficiencies.	24
2.3	Equivalent circuit of the battery	26
2.4	Scheme and free body diagram of the TCD	27
3.1	<i>P2P4</i> layout representation	32
3.2	P2P4s layout representation	33
3.3	Representation of the metamap	37
3.4	Working points in CS operation represented in the Metamap	40
3.5	Representation of battery charging/depleting working points on the metamap	41
4.1	WHVC cycle.	46
4.2	CO ₂ emissions vs Degrees of freedom of the vehicle.	48
4.3	CO ₂ emissions vs Degrees of freedom of the vehicle.	49
4.4	Detail of the diving mission performed in battery charging mode.	50
4.5	Detail of the diving mission performed in charge sustaining mode.	51
4.6	Optimal SOC and powerflow profiles on the driving mission	51

Chapter 1

Introduction

1.1 Introduction to hybrid vehicles

The research of novel propulsion systems for the transport sector represents a demanding challenge for the automotive sector, aimed at reducing the emissions of pollutants and CO_2 gases according to new regulations [2]. In particular, hybrid vehicles shows effective reductions in terms of engine emissions with respect to a conventional vehicle [3] [4], especially on urban driving segments where the reductions of CO_2 emissions and fuel consumption are up to 40% and 65% respectively [5].

The main advantage of electric vehicles is represented by the possibility to implement a further energy conversion in the processes that involve the production of energy with respect to conventional vehicles. In fact, the chemical energy stored in the fuel and converted into mechanical energy by the internal combustion engine is not immediately exploited, and a further conversion of energy from mechanical into electrical is present. This electrical energy can be stored in the vehicle by means of batteries and capacitors and successively used for traction. As a consequence, in pure electric mode the vehicle does not generate any form of pollutant. In the case of vehicles that feature only electric components for traction, the electricity that is contained in the battery is produced in an external plant, that is able to control the production more efficiently with respect to a internal combustion engine of a conventional vehicle. In the case of hybrid vehicles, that feature both an internal combustion engine and a battery with generators, it is possible to obtain different traction configurations by combining the two energy sources. More in details, the vehicle can mainly behaves in three ways:

- pure electric, when only the battery is used as energy source
- pure thermal, when only the internal combustion engine is used as energy source
- hybrid mode, when the battery and the internal combustion engine work simultaneously in order to propel the vehicle

Hybrid vehicles feature the possibility to exploit the phenomenon of regenerative braking, that allows the conversion of kinetic energy of the vehicle during braking phases

into electrical energy to be stored in the battery. This procedure is possible by means of the electric machine installed in the powertrains. More in details, electric machines are reversible components, hence they are able to convert electric energy into mechanical (motor configuration) and mechanical energy into electric (generator configuration). During braking phases the electric machine works as generator: the energy that is required to brake, usually dissipated into thermal energy in a conventional vehicle, is partially recovered into electric energy and stored in the battery.

The development of hybrid vehicles with different strategies and techniques led to various typologies of solution [6]. A possible distinction can be made according to the *Hybridization Factor* (HF) defined as the ratio of the maximum energy that the vehicle is able to supply using electric components over the total maximum energy that can be delivered by using both electric components and the internal combustion engine. The different hybridization levels are [7]:

- *Micro HEVs*: are vehicle that feature a small electric machine that solves the same functions of a starter motor and a alternator. This electric machine is used to switch off the internal combustion engine when needed, e.g. during stops, and to switch it on when starting signal is received. The power required to propel the vehicle is provided only by the internal combustion engine.
- *Mild HEVs*: the layout of this category of vehicle is similar to ones of the category described above. In this case, the electric machine is equipped with a small battery. The electric machine solves the function of aiding the internal combustion engine during peak power requests. This hybrid vehicles permit considerable savings with respect to conventional vehicles in terms of fuel consumption [8].
- *Full HEVs*: this family of hybrid electric vehicles is equipped with a larger electric machine with respect to the two categories listed above; in this case pure electric mode can be obtained, and the internal combustion engine size is consequently smaller.
- *Plug-in HEVs*: this family of hybrid vehicles, also called PHEVs, features the presence of a plug that is connected with the battery. This layout permits battery recharges directly from the electric distribution network. As a consequence, PHEV vehicles are capable of a wide pure electric range [9].

1.2 Classification of hybrid vehicles

Traditionally [10], hybrid vehicles are classified according to the energy fluxes that the vehicle is capable to manage. These fluxes of power are generated by the two main sources of energy, represented by the internal combustion engine and the electric generators. The power fluxes are directed towards the powertrains, and they can be divided by means of torque coupling devices and electric circuits. The four main layout categories are: series HEVs, parallel HEVs, series-parallel HEVs and complex HEVs.

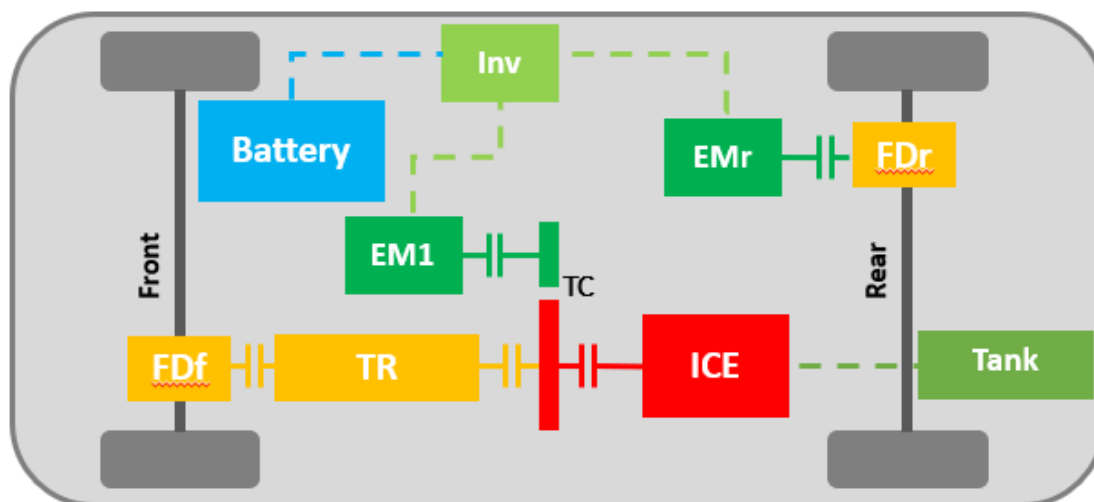


Figure 1.1. Parallel Double Shaft hybrid vehicle.

1.2.1 Series hybrid vehicles

In series electric vehicles, the internal combustion engine is disengaged from the transmission. The traction is provided by the electric machine only that can be mounted on the rear or frontal powertrain. A second electric machine is present in series hybrid vehicles, that represent the generator, and it is connected with the internal combustion engine. The generator converts mechanical energy supplied by the internal combustion engine into electrical energy, that can flow into the battery or towards the powertrain by the means of a power converter.

The series configuration represents the object of the present study; the proposed layout is described in details in chapter 3 as well as the implementation of the optimization tool is described in chapter 2.

1.2.2 Parallel hybrid vehicles

The architecture of a parallel hybrid vehicle is generally equipped with a single electric machine, that can be mounted either on the rear powertrain or on the frontal powertrain, according to the desired layout. The main source of energy is represented by the internal combustion engine, while the electric machine accomplishes the task of assisting the traction phases by the means of a torque coupling device. The main difference of a parallel with respect to a series architecture is represented by the fact that the energy conversion occurs in a minor extent during the stages between the sources of energy and the vehicle wheels (figure 1.2.2). Consequently a parallel hybrid vehicle is characterized by a higher overall efficiency in the management of power.

Parallel HEVs can be further classified into:

- *Double Drive*, where both the axles of the vehicle are served with a dedicated powertrain.
- *Double Shaft*, where only an axle of the vehicle is served, and it features the presence of a double transmission. Each transmission is linked to a different power source.
- *Single Shaft*, where only an axle of the vehicle is served. The mechanical power that comes from different sources is coupled before the transmission.

Parallel HEVs' main advantage is the adaptability to different driving conditions due to the widespread possibilities in energy flow management. This feature permits to obtain three different working mode of the vehicle, that are:

- pure electric, where the electric machine provides all the traction required for the advancement and the internal combustion engine is switched off.
- pure thermal, where the internal combustion engine provides all the traction required for the advancement and electric machine is switched off.
- hybrid traction or *powersplit*, where both the internal combustion engine and the electric motor contribute to satisfy the request of power required by the vehicle.

1.2.3 Series-parallel hybrid vehicles

The series-parallel layout, represented in figure 1.2.3, combines the advantages of series HEVs and parallel HEVs architectures. This layout is characterized by the presence of two point in which the power fluxed are coupled. More in details, the first point is represented by the power converter that join the generator with the battery and the electrical motor. The second point is situated downstream the mechanical transmission and is represented by a torque coupling device, that join the mechanical power produced by the internal combustion engine and the mechanical power that comes from the electric motor. The possible working modes that the vehicle is capable to provide are: pure electric, pure thermal, parallel mode and series mode. In the parallel mode the power flows are identical to the ones described in the parallel HEVs paragraph; this configuration is obtained thanks to the mechanical clutch equipped between the generator and the power split device. More in details, the clutch separates the mechanical power flux between the internal combustion engine and the generator. The series mode is vice versa obtained using the clutch to mechanically couple the internal combustion engine with the electric machine, that works as generator. In this case, a second clutch is used to separate the mechanical flux coming from the internal combustion engine and the powertrain.

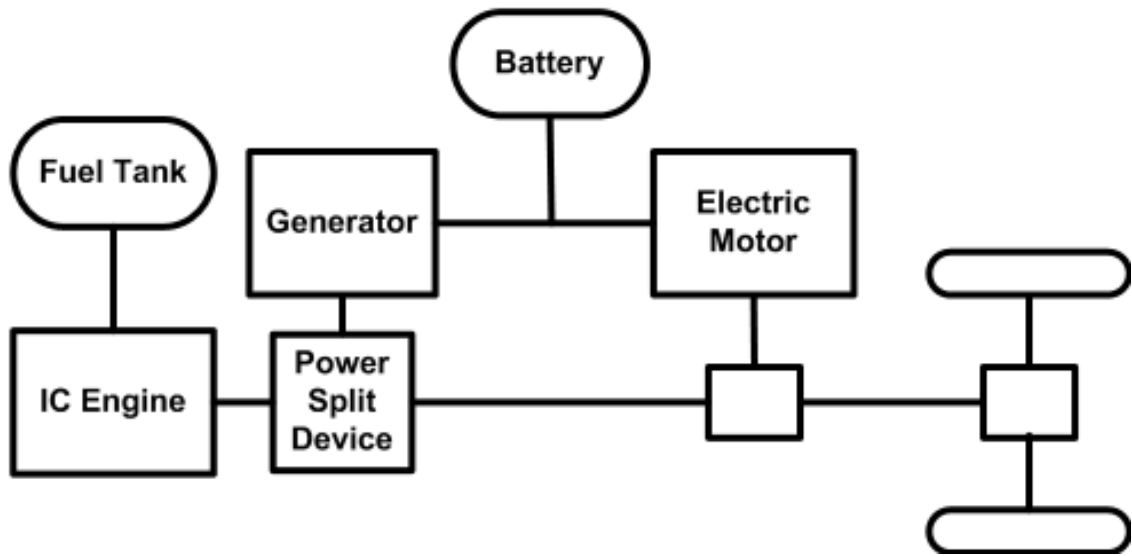


Figure 1.2. Series-parallel layout.

1.2.4 Electric machines position classification

A possible distinction of hybrid vehicles (that feature one or more electric machines that can provide pure electric traction) can be also made according to the position of the electric machines in the vehicle:

- P1f or P0: the electric machine is connected to the engine, in the position of the alternator.
- P1r: the electric machine is directly coupled with the crankshaft, in intermediate position between the ICE and the transmission.
- P2: the electric machine is equipped between the clutch and the transmission.
- P3: in this layout the electric machine is mounted downstream the transmission.
- P4: in this case the electric machine is mounted on the rear powertrain.

Chapter 2

Concept and Design of an Optimization Tool for HEVs

The present chapter describes the concepts of an *optimization tool* designed for hybrid electric vehicles, on the basis of aimed to the research and the definition of an absolute optimal control strategy that can be exploited on a hybrid architecture in order to minimize a desired objective function over a specific mission of the vehicle. To this end, the tool exploits a deterministic dynamic programming algorithm, that represent a consolidated technique to approach the problem [11][12].

The user can choose the vehicle mission for the optimization arbitrarily, such as the objective function to be minimized for the optimal control strategy definition and all the specific details to run the vehicle simulation.

2.1 Dynamic programming optimization

Dynamic programming is a method which aims to find the absolute optimal policy for a multi-stage decisional making problem, which is discretized over N stages. It is a common tool that finds widespread applications among engineering, physics and economics problems. The system is characterized by a state, which evolves in time according to the decisions or controls which are taken at each stage. The objective is to minimize a cost function which is considered an undesirable outcome of the system. The dynamic programming provides, as result, the optimal rule for selecting, at each stage k , a decision or control for each possible value of the state of the system than can possibly occur. This is a more general and powerful solution than finding the precise set of subsequent decisions which have to be taken, because the dynamic programming, by providing us the rules to be followed in the specific problem which is analysed, allows as to be always able to find the optimal sequence of decisions, regardless what the initial state of the system will be.

The term *dynamic* refers to the fact that the system can evolve in time according to its own physical laws. The system is generally characterized by the following variables:

- state variables
- decision (or controls)
- external variables

2.1.1 Cost-to-go function

The cost-to-go function is the objective function which the dynamic programming aims to minimize over the entire time mission. The total cost is defined as:

$$J_{tot} = C_N(x_N) + \sum_{k=0}^{N-1} C_k(x_k, u_k, w, k) \quad (2.1)$$

where $C_N(x_N)$ is the final cost at the stage N, $C_k(x_k, u_k, w, k)$ is the instantaneous transition cost at the time instant t_k , x_k , u_k and w_k are the vectors of state, controls and external variables at time t_k respectively.

2.1.2 Deterministic problems

A problem is said to be deterministic if, given the state of the system at the generic time t_k , by choosing a specific control u_k , the state of the system at the time $t_k + 1$ is uniquely identified. This means that, if the problem is deterministic, if the system is in a well-defined state and a defined control strategy is taken, the state of the system evolves in a precise way and the final state of the system will be unique.

2.1.3 Optimal policy definition

A *policy* is any rule for making decisions which yields an allowable sequence of decisions. An *optimal policy* is a policy which minimizes a preassigned function of the final state variables, denoted cost-to-go function. The definition of an optimal policy is extremely general, because it contains the rules that any system has to follow in order to evolve through the best decisions stage by stage, regardless of which the state of the system is at the beginning of the system mission.

The optimal policy is found by the dynamic programming through the *principle of optimality*, stated by Richard Bellman [13]:

"An optimal policy has the property that whatever the initial state and initial decision are, the remaining decisions must constitute an optimal policy with regard to the state resulting from the first decision"

that it mathematically expressed by the truncated solution $u_{opt,t}$ of equation 2.1 which is defined over the stages $t, \dots, N - 1$. Hence the optimal solution for minimizing the truncated cost function J_t is:

$$J_t = C_N(x_N) + \sum_{k=t}^{N-1} C_k(x_k, u_k, w, k) \quad (2.2)$$

2.1.4 Algorithm

The Dynamic Programming algorithm solves the problem in two phases:

- a backward phase
- a forward phase

Backward phase

The dynamic programming starts to operate from the last stage of the problem. The cost function is initialized at the last stage, as a function of the state of the system at the last stage. In other words, the final cost $C_N(x_N)$ at the stage N is known.

At the specific stage t_k , the optimal cost-to-go function is $J_{opt}(x_k)$, which is the optimal cost if, at stage k, the system follows the optimal control strategy from stage k to stage N, starting from the state x_k . The optimal cost function $J_{opt}(x_k)$ can be obtained on the basis of the previously computed cost function at the stage $t_k + 1$, by solving the minimization problem expressed as:

$$J_{opt}(x_k) = \min (J_{opt}(x_k + 1) + C_k(x_k, u_k, w_k)) \quad (2.3)$$

This problem is only a function of the control u_k which can be chosen at the time instant t_k . By solving the problem at the stage t_k , the result of the algorithm is the best control u_k that can be chosen for each possible initial state x_k . This procedure is iterated until the first stage is reached.

The result of the backward phase is the optimal policy of the studied problem. The optimal policy computed by the dynamic programming, describes which is the best decision that must be taken at each time $t_k(0 \leq k \leq N - 1)$ for each possible state of the system x_k that might occur. Therefore, the result of the backward phase can be considered as the main (and general) result of the dynamic programming since it optimally describes the entire problem: regardless of the initial state of the system at time t_0 , the system optimal trajectory is known by means of optimal controls that minimize the undesired cost function.

Forward phase

The forward phase is just a consequence of the previous backward phase and it can be considered as the application of the optimal policy to the specific case which is studied. The user knows the initial state of the system x_0 at the time t_0 and, following the optimal policy, he knows which control must be chosen at the first stage. This control will lead to an evolution of the state of the system to the state x_1 . On the basis of the state x_1 , the user chooses the best control for the second stage, always according to the previously computed optimal policy. This procedure is iterated until the last stage is reached. The result of the forward phase will be the set of controls $u = \{u_0, u_1, \dots, u_{N-1}\}$ which must be chosen by the user stage by stage during the

system mission, in order to minimize the undesired cost function, when the initial state of the system x_0 is known at the initial time t_0 .

2.2 Time discretization

The vehicle performances are investigated through particular driving missions as consequences of the application of specific controls. A discretization of the time domain in N_{in} intervals and $N_{in} + 1$ nodes is applied on each driving mission, thus leading to a description of the system by means of discrete variables.

In this study an *interval – grid* approach is used, in which the mission is divided in adequately long intervals. Control variables are set to be constant over the single time interval, while the system quantities are evaluated at the begin and at the end of each interval. The values of the system quantities along the interval are then calculated through interpolation. Being sv a system variable, obtained as a function of n_c number of control variables and n_s number of system variables, it is possible to write:

$$sv_l(i) = f(cv_1(i), \dots, cv_{n_c}(i), sv_{1,l}(i), \dots, sv_{n_s,l}(i)) \quad (2.4)$$

$$sv_r(i) = f(cv_1(i), \dots, cv_{n_c}(i), sv_{1,r}(i), \dots, sv_{n_s,r}(i)) \quad (2.5)$$

where i is the generic time interval, sv_l and sv_r are the values of the system variable associated respectively to the left and right ends of the intervals. Hence the relation

$$cv_{j,r}(i) = cv_{j,l}(i) \quad (2.6)$$

is valid for the generic control variable cv_j over the interval i . Is it possible to obtain the formulation of the derivative of state variables associated to the outer nodes of intervals as:

$$\frac{dsv_l(i)}{dt} = \frac{dsv_r(i)}{dt} = \frac{sv_r(i) - sv_l(i)}{\Delta t} \quad (2.7)$$

and the formulation of the integral as:

$$\left(\int_{\Delta t} sv_l \right) (i) = \left(\int_{\Delta t} sv_r \right) (i) = \frac{sv_r(i) + sv_l(i)}{2} \cdot \Delta t \quad (2.8)$$

A different approach would be the *node – grid* one, in which each control variable, state variable and physical quantity is associated to a node i of the grid. The previous equations become:

$$sv(i) = f(cv_1(i), \dots, cv_{n_c}(i), sv_1(i), \dots, sv_{n_s}(i)) \quad (2.9)$$

while the expression of the derivative becomes:

$$\frac{dsv(i)}{dt} = \frac{sv(i) - sv(i-1)}{\Delta t} \quad (2.10)$$

and the expression of the integral can be written as:

$$\left(\int_{\Delta t} sv\right)(i) = \frac{sv(i) + sv(i-1)}{2} \cdot \Delta t \quad (2.11)$$

This *node-grid* approach is however not adopted in the present study. A poor refined grid would indeed not represent correctly the evolution of the physical quantities along the driving mission, especially the ones that require an integration over the interval of time, such as the output values of the state of charge of the battery or the consumption. A too refined grid would on the contrary preserve the precision of the estimations of the integrals and derived quantities, although increasing drastically the computational time required by the program.

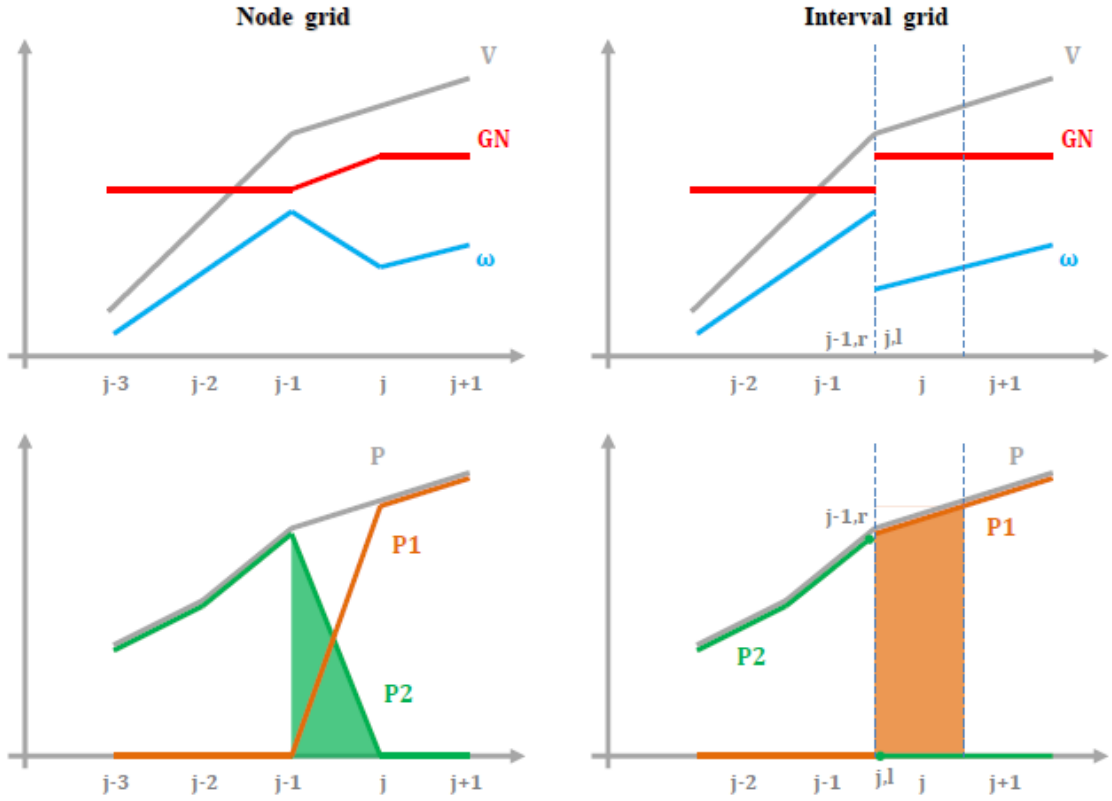


Figure 2.1. Discretization of time domain

Figure 2.2 shows the comparison between *node-grid* and *interval-grid* approach. From the graphs in the first row it is possible to observe how discrete values of state variables (gear number in the example) are preserved with the *interval-grid* approach. A similar description of the system would be possible also with a *node-grid* approach with a thin mesh refinement.

The graphs on the second row of figure 2.2 show the behaviour of an integral variable instead, namely the power provided by the motor. The power along a certain interval is obtained using the trapezoidal rule, namely the subtended area of the function evaluated in two consecutive nodes. The problem of this approach is the lack precision of the result in case of switching on/off of the motor, leading to underestimation (when the motor is switched on) and overestimation (when the motor is switched off) of the power output. Again this issue can be overcome by means of a mesh refinement in case of *node-grid* approach, while a *interval-grid* approach would preserve computational accuracy by introducing r and l values for each node.

Concluding, it is worth noticing that the duration of intervals (and so the node grid refinement) in the *interval-grid* approach does not affect the precision of the evaluation of integral variables and intermediate variables. The presence of a wide time interval only affects the optimized solution, since controls over the vehicle are kept constant for a longer period of time.

2.3 Input variables

The input variables are the information about the vehicle mission where the control strategy has to be optimized. The input variables are:

- the vehicle velocity V_v
- the slope of the road α

These two information are then processed by the tool; more in detail a kinematic model and a dynamic model assess for the feasibility of the vehicle to be successfully driven in such conditions. Velocity of the vehicle V is estimated at the begin and at the end of each interval and then stored in column vectors, hence

$$V_{v,r}, V_{v,l} \in \mathbb{R}^{N_{in} \times 1} \quad (2.12)$$

where N_{in} are the number of intervals of the mission. The same procedure holds for the road slope α .

2.4 Control variables

The control variables cv are the parameters that have to be properly chosen over the mission to minimize the desired objective function. The generic control variable cv_i can assume discrete values, and sub-control variables $scv_{i,j}$ are parameters that are associated to the relative control variable. The control variables are :

- the gear number GN
- the power flow PF

The gear number GN describes the number of transmission gear of the vehicle. It controls the values of the sub-control variable transmission ratio τ . The set of GN is defined as:

$$S_{gn} = \{1, \dots, N_{gn}\} \quad (2.13)$$

where N_{gn} is the total number of GN parameters.

The power flow PF describes the power split among different components by the vehicle. The set of PF is defined as:

$$S_{pf} = \{1, \dots, N_{pf}\} \quad (2.14)$$

where N_{pf} is the total number of PF. This number is not immediately obtained as in the case of N_{gn} as total gears present in the transmission. In fact, the power management in a hybrid vehicle may be very complex and it depends on its architecture(i.e. the number electrical machines and their position on rear or frontal axes,...). Two sub-control variables are hence introduced in order to define mathematically the power flow in an unequivocal way:

- the sub-control variable α : it computes the ratio between the power provided by the battery to the frontal axle and the frontal power demand of the vehicle
- the sub-control variable ϕ : it computes the ratio between the power supplied by the rear axle and the total power demand.

The space of the control variables is then defined as:

$$S_{cv} = S_{gn} \times S_{pf} \quad (2.15)$$

More in detail, the product between all the possible discrete values of the control variables GN and PF represents the working modes of the vehicle. Hence, a singular control applied on the vehicle over the generic time interval is characterized by a specific value of GN and PF.

2.5 State variables

The state variables sv are parameters that describes possible conditions of the vehicle over the mission.

The first sv is the engine state ES. The set of ES is defined as:

$$S_{es} = 1, \dots, N_{es} \quad (2.16)$$

where N_{es} is the number of possible engine states, that are:

- $ES = 0$ when the engine is switched off
- $ES = 1$ when the engine is switched on

The ES number can be directly obtained in relation to the working modes described in the previous paragraph.

The second sv refers to the state of charge of the battery, i.e. the SOC. The possible values that the SOC can assume are represented by the SOC grid that is included in the SOC window, ranging from SOC_{min} and SOC_{max} with step ΔSOC . The number of the nodes of the SOC grid N_{soc} are

$$N_{soc} = \frac{SOC_{max} - SOC_{min}}{\Delta SOC} + 1 \quad (2.17)$$

The sv SOC is hence represented by its grid, and the set is defined as:

$$S_{soc} = \{1, \dots, N_{soc}\} \quad (2.18)$$

where N_{soc} has been evaluated by means of 2.17.

2.6 Configuration matrices approach

The pre-processing phase of the tool is aimed at arranging input variables, control variables, intermediate variables and state variables in particular structures called configuration matrices (CM). This technique have been adopted in order to reduce the computational time needed to find the optimal control strategy with the optimization algorithm.

The set of configurations is introduced as the Cartesian product of the following sets:

$$S_{conf} = S_{gn} \times S_{pf} \times S_{es} = S_{wm} \times S_{es} \quad (2.19)$$

the corresponding number of configurations of the problem N_{conf} is therefore obtained as:

$$N_{conf} = N_{gn} \times N_{pf} \times N_{es} = N_{wm} \times N_{es} \quad (2.20)$$

Being v the generic variable, the associated configuration matrix belongs to the domain:

$$M_v \in \mathbb{R}^{N_{in} \times N_{conf}} \quad (2.21)$$

where N_{in} number of intervals is equal to the number of rows and N_{conf} number of configuration is equal to the number of columns. For each variable v , two configuration matrices are built according to the interval-grid approach: $M_{v,l}$ and $M_{v,r}$, that are respectively the configuration matrices at the begin and at the end of each interval.

2.7 Intermediate variables

Once the tool is fed with the driving mission, i.e. the values of input variables, and the space of control variable is set, some computations are required in the pre-processing stage in order to obtain additional parameters that are needed to describe the vehicle behaviour along the simulation. Such derived quantities are called intermediate

variables, and they mainly refer to the components' speed and power. Despite the diversity of HEV architectures, and the necessity to assess to a dedicated model for each of them, a common line of derivation is present and shown in this paragraph.

The total vehicle power demand P_v can be estimated from input variables as:

$$P_v = P_{v,roll} + P_{v,grade} + P_{v,inertia} + P_{v,drag} \quad (2.22)$$

The term $P_{v,roll}$ takes into account the power requested to overcome the rolling resistance of the wheels and it is computed as:

$$P_{v,roll} = (m_v \cdot g \cdot r_v \cdot \cos \alpha_r) \cdot V_v \quad (2.23)$$

where m_v is the vehicle mass, g is the acceleration of gravity, α_r is the slope of the road and r_v is the rolling resistance coefficient.

The term $P_{v,grade}$ accounts for the vehicle weight component projected along the driving direction. It is computed as:

$$P_{v,grade} = (m_v \cdot g \cdot \sin \alpha_r) \cdot V_v \quad (2.24)$$

The term $P_{v,inertia}$ represents the vehicle and wheels inertia and it is computed as:

$$P_{v,inertia} = \left(m_v + \frac{I_{wh}}{R_{wh}} \right) \cdot \dot{V}_v \cdot V_v \quad (2.25)$$

where I_{wh} is the wheel inertia, R_{wh} is the dynamic wheel radius and \dot{V}_v is the punctual vehicle acceleration.

The term $P_{v,drag}$ accounts for the total drag resistance power and is expressed as follows:

$$P_{v,drag} = \left(\frac{1}{2} \cdot \rho_{air} \cdot c_x \cdot A_v \cdot V_v^2 \right) \cdot V_v \quad (2.26)$$

where A_v is the frontal area of the vehicle, ρ_{air} represents the air density and c_x is the aerodynamic drag coefficient.

When the value of P_v is positive, the vehicle is in *traction* phase. In this case the power at the road level P_v is split among front wheels and rear wheels, accounted in the terms $P_{wh,f}$ and $P_{wh,r}$ respectively. Their expression is:

$$P_{wh,f} = (1 - \phi) \cdot P_v \quad (2.27)$$

$$P_{wh,r} = \phi \cdot P_v \quad (2.28)$$

where ϕ is the sub-control variable of the PF that describes the amount of power split. When P_v is negative, the vehicle is in *braking* phase. The following equation are then used:

$$P_{wh,f} = \gamma_{fr} \cdot P_v \quad (2.29)$$

$$P_{wh,r} = (1 - \gamma_{fr}) \cdot P_v \quad (2.30)$$

being γ_{fr} the factor that represents the power split among axes during the braking phase.

The power at the final drives $P_{fd,f}$ $P_{fd,r}$ (front and rear respectively) are hence evaluated. During the traction phase they are equal to:

$$P_{fd,f} = P_{wh,f} \quad (2.31)$$

$$P_{fd,r} = P_{wh,r} \quad (2.32)$$

introducing then γ_{br} as the power fraction dissipated due to friction, the following expressions holds for the braking phase :

$$P_{fd,f} = (1 - \gamma_{br}) \cdot P_{wh,f} \quad (2.33)$$

$$P_{fd,r} = (1 - \gamma_{br}) \cdot P_{wh,r} \quad (2.34)$$

Finally the quantities of power requested by the frontal powertrain $P_{req,f}$ and the rear powertrain $P_{req,r}$ are:

$$P_{req,f} = (P_{fd,f} + P_{in,tr}) \cdot \eta_{tr}^k + P_{in,em} + P_{ice,in} \quad (2.35)$$

$$P_{req,r} = P_{fd,r} + P_{in,emr} \quad (2.36)$$

where $P_{in,tr}$, $P_{in,em}$, $P_{ice,in}$ are the inertial power of transmission, electrical machine and engine respectively and they are evaluated at each time interval as:

$$P_{tr,in} = I_{tr} \cdot \dot{\omega}_{tr} \cdot \omega_{tr} \quad (2.37)$$

$$P_{em,in} = I_{em} \cdot \dot{\omega}_{em} \cdot \omega_{em} \quad (2.38)$$

$$P_{ice,in} = I_{ice} \cdot \dot{\omega}_{ice} \cdot \omega_{ice} \quad (2.39)$$

2.8 Optimization phase

The optimization phase begins after the pre-processing phase, that was dedicated to the description of the system through the configuration matrix approach. More in details, the dynamic programming algorithm that is used in the present study is *deterministic*, hence all the physical quantities that are needed to describe the vehicle must be computed a priori. The optimal control strategy of the vehicle is obtained as a result from the optimization phase, namely the set of controls on the vehicle during the driving mission that lead to the minimization of the fuel consumption.

The optimization procedure is divided in backward phase and forward phase. The backward phase begins at the last interval of the time domain of the driving mission. A new grid is created, defined as combination of the two state variables of the vehicle, namely engine state ES and state of charge SOC. For all the possible combinations of engine state and SOC, a score function ψ is initialized as follows:

- $\psi = \infty$ for each point of the grid such that the SOC is larger than the initial SOC of the vehicle mission and the engine is off.

- $\psi = 0$ otherwise.

Then, for each point of the grid the tool computes the fuel consumption ϵ in the last interval by reading the instantaneous fuel consumption at the beginning and at the end of the last interval from the configuration matrices and performing an integration over that time interval. This value ϵ is used to update the score function, that becomes:

$$\psi^* = \begin{cases} \psi(j) + \epsilon_j, & \text{if } SOC_{min} < SOC(j) < SOC_{max} \\ \infty, & \text{otherwise} \end{cases} \quad (2.40)$$

Being j the generic time interval. The tool selects the best combination of control variables to use at the last interval for each possible combination of state variables at the end of the previous interval and the corresponding updated score. This procedure is repeated until the first interval is reached.

In the forward phase, the tool selects the optimal control strategy, namely powerflow PF and gear number GN, that leads to the final stage according to the initial conditions imposed on the vehicle, namely the initial value of the SOC.

2.9 Vehicle components

2.9.1 Internal combustion engine

Hybrid vehicles features smaller internal combustion engine with respect to conventional vehicles, in order to enhance the efficiency and reduce fuel consumption. In the present study a compression ignition engine is considered, powered by diesel fuel. The engine performances are modelled using tables data derived from tests. The fuel consumption mass flow rate is computed as a function of rotating speed and torque, on a basis of a two dimensional map:

$$\dot{m}_f = f(\omega, T) \quad (2.41)$$

the consequential value of carbon dioxide that is emitted is obtained as follows:

$$C\dot{O}_2 = 2,65 \cdot \frac{\dot{m}_f}{\rho} \quad (2.42)$$

where ρ is the air density.

2.9.2 Electric machine

The electrical components that are responsible for the propulsion are electrical machines (EM), power inverters and controllers. Electrical machines accomplish the function of delivering mechanical power to propel the vehicle. The EM also process the power flow in the reverse direction, when the vehicle is braking, converting mechanical energy coming from the rotating wheels into electrical energy to be stored in the battery. In the first case, when the power is converted from electrical to mechanical, the

EM works as motor. In the second case, when the power is converted from mechanical to electric, the EM works as generator. Popular electrical machines suitable for hybrid vehicle application are either asynchronous or permanent magnet (PM). Nowadays, permanent magnet machines are getting more widespread in traction applications due to their superior power density, compactness and current availability of power electronics needed for effective control. Another important component that serves the electrical propulsion system is the power converter. The power converter delivers the power to the electrical machine with appropriate values of voltage and current.

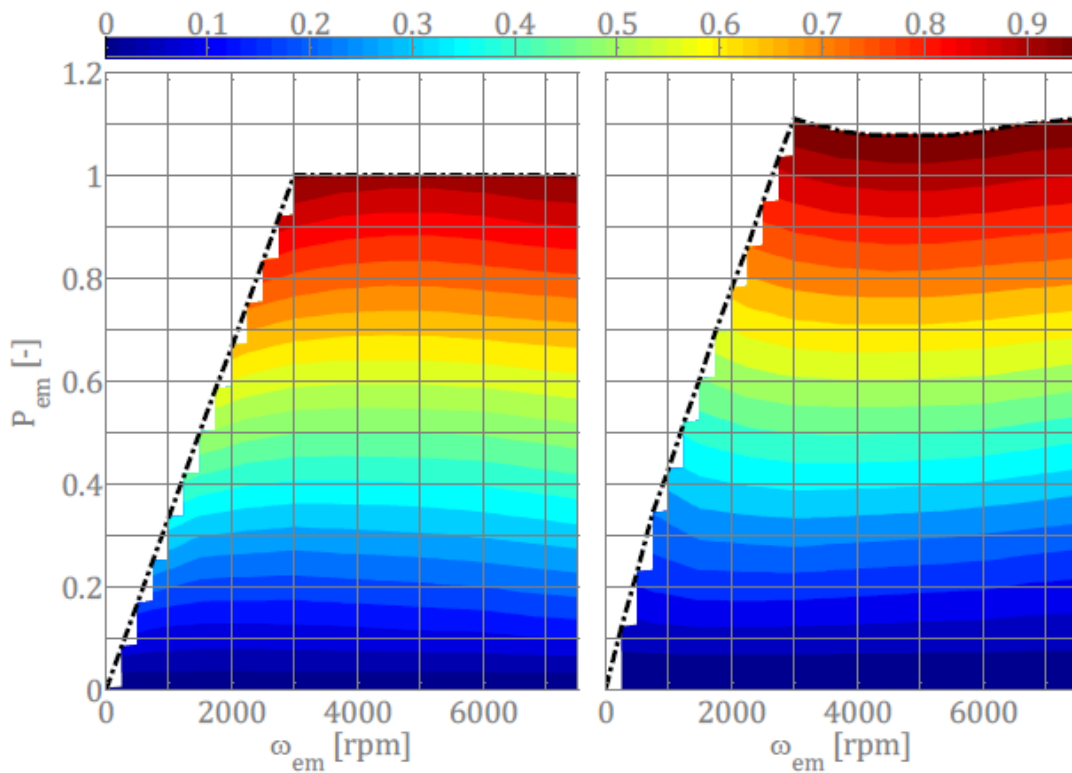


Figure 2.2. Electric machine conversion efficiencies.

In this study, the employed EM is a brushless PM. The main features of this kind of electrical machines are high efficiency, robustness and simple layout. On the other hand, they are quite expensive due to the magnets' cost. Figure 2.9.2 shows the normalized efficiencies values of EM in case of mechanical to electric conversion (left) and electric to mechanical conversion (right).

2.9.3 Battery

In the present work, lithium-ion batteries are considered as electrochemical power storage devices. The Optimization Tool used to develop the study embeds a sizing procedure for the battery. The first value computed is the maximum power of the battery $P_{batt,max}$, estimated from the the size of the electrical machines employed in the vehicle and their maximum deliverable power. Then the total number of battery cells $N_{cell,tot}$ is computed as follows:

$$N_{cell,tot} = N_{cell,p} \cdot N_{cell,s} \quad (2.43)$$

where $N_{cell,p}$ is the number of cell in parallel and $N_{cell,s}$ is the number of cell in series. The singular reference cell properties are summarized in the following table: Being

Cell properties	
$m_c[kg]$	0.2
$V_c[V]$	3.6
$R_c[Ohm]$	0.002
$C_c[Ah]$	5.5
$I_{c,max}[A]$	120
$SOC_{max}[-]$	0.8
$SOC_0[-]$	0.6
$SOC_{min}[-]$	0.4
$\lambda[Ah]$	150 000

Table 2.1. Elementary cell properties

$I_{c,max}$ the maximum current of a cell, V_c the maximum voltage and R_c the resistance, the total number of cells can be obtained as:

$$N_{cell,tot} = \frac{P_{max}}{V_c \cdot I_{c,max} - R_c \cdot I_{c,max}^2} \quad (2.44)$$

The following expressions are then used to compute the number of cells in parallel and in series:

$$N_{cell,p} = \frac{N_{cell,tot} \cdot V_c}{500} + 1 \quad (2.45)$$

$$N_{cell,s} = \frac{N_{cell,tot}}{N_{cell,p}} \quad (2.46)$$

Nominal properties of the battery are finally computed and represented in the equivalent circuit in figure 2.9.3:

$$R_{bat} = R_c \cdot N_{cell,s} \quad (2.47)$$

$$V_{bat} = V_c \cdot N_{cell,s} \quad (2.48)$$

$$C_{bat} = C_c \cdot N_{cell,p} \quad (2.49)$$

$$E_{bat} = C_{bat} \cdot v_{bat} \quad (2.50)$$

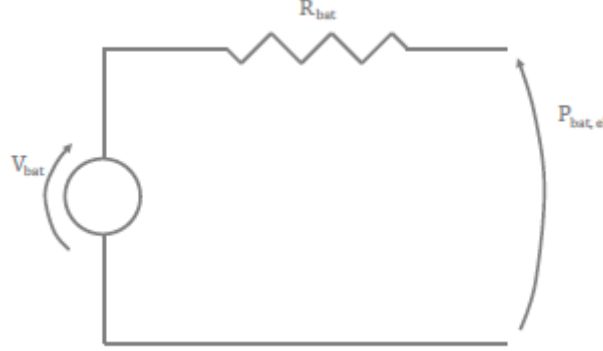


Figure 2.3. Equivalent circuit of the battery

During the pre-processing phase of the optimization, the power to be managed by the battery is computed at each time step. Being $P_{i,el}$ the electric power flow associated with the generic electric machine and η_{inv} the efficiency of the inverter, the energy balance of the battery is:

$$P_{bat,el} = \sum_{i=1}^n P_{i,el} \cdot \eta_{inv}^k \quad (2.51)$$

where n is the number of electrical machines. The overall energy is obtained as result of the algebraic sum of the singular contribution. When this value is positive, it means that the battery is discharging. In this case $k = -1$, hence the sum of the power required by all the electric machines on board divided by the efficiency of the inverter. In the opposite case $k = 1$, and the sum of the power provided by all the electric machines multiplied by the efficiency of the inverter.

By referring to the equivalent circuit of figure 2.9.3, it is possible to derive all the physical quantities that leads to the estimation of the battery SOC. The chemical power requested to the battery is equal to:

$$P_{bat,chem} = V_{bat} \cdot I_{bat} = P_{bat,el} + R_{bat} \cdot I_{bat}^2 \quad (2.52)$$

It is possible to derive the instantaneous current as follows:

$$I_{bat} = \frac{V_{bat} - \sqrt{V_{bat}^2 - 4 \cdot R_{bat} \cdot P_{bat,el}}}{2 \cdot R_{bat}} \quad (2.53)$$

And finally the value of the SOC, representing the state of charge of the battery referred to the fully charged battery, as;

$$SOC = SOC_0 - \int \frac{I_{bat}}{C_{bat}} \cdot dt \quad (2.54)$$

2.9.4 Torque coupling device

The Torque Coupling device (TCD) is a mechanism that is used to join the torques coming from the electrical machine and the internal combustion engine, that lays on two different shafts, into a single output shaft of the transmission. Moreover, the torque coming from the internal combustion engine can also be split in two output through the TCD: one flows into the transmission and the remaining part flows into the electrical machine in order to generate electrical power during the battery charging mode.

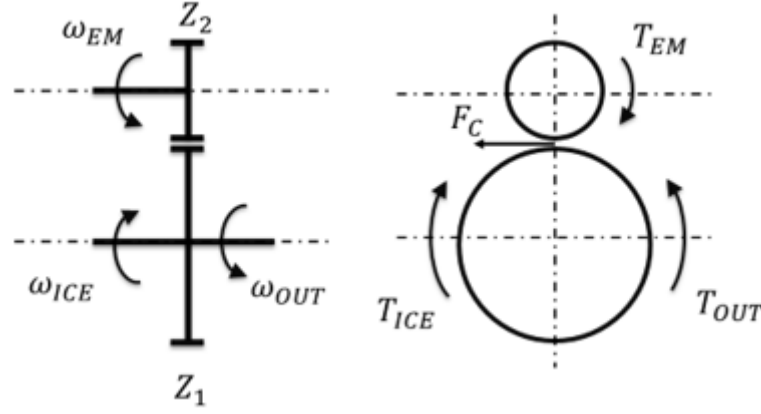


Figure 2.4. Scheme and free body diagram of the TCD

The figure 2.9.4 reports the scheme of a TCD (left) and an example of a free body diagram (right). Z_1 and Z_2 represent the number of teeth of gear 1 and gear 2 that are part of the device, F_c is the contact force. With respect to figure 2.9.4 it is possible to write the following relations:

$$\omega_{ice} \cdot Z_1 = \omega_{out} \cdot Z_1 = \omega_{EM1} \cdot Z_2 \quad (2.55)$$

$$\tau = \frac{Z_1}{Z_2} \quad (2.56)$$

$$F_c = \frac{T_{EM1}}{R_2} \quad (2.57)$$

Where R_2 is the primitive pitch of gear 2, and τ is the speed ratio. From equation 2.55 it is possible to write the expression of the shafts as:

$$\omega_{out} = \omega_{ICE} = \frac{\omega_{EM1}}{\tau} \quad (2.58)$$

and from the equilibrium to rotation of gear 1:

$$T_{out} = T_{ICE} + F_c \cdot R_1 = T_{ICE} + \frac{T_{EM1}}{R_2} \cdot R_1 = T_{ICE} + T_{EM1} \cdot \tau \quad (2.59)$$

Chapter 3

Series architecture implementation

The series HEV configuration particularly suitable for those applications characterized by a high ratio between the peak of power required for traction and the mean power required along the mission, as well as the driving mission with frequent acceleration and braking phases, and the ones in which long stops are present [10].

In those stops, the ICE, under the conditions of fixed working point, i.e. constant angular speed, it is able to recharge the batteries, even partially, providing power in a minor extent with regards to the power levels requested during the traction phase. In this way, the vehicle is permitted to travel long distances in pure electric mode. This is the typical case of the mission of a urban public transport bus.

The advantages offered by a series traction layout are, in addition to the ones typical of hybrid vehicles in terms of reduction of emission of pollutants and consumption:

- The components belonging to the traction system are all small sized and not rigidly connected one with the other. Is it then possible to separate the components and dispose them in appropriate points in the vehicle in order to optimize the mass distribution and an enhancement of exploitable space.
- The effects of vibrations and noises coming from the ICE are reduced. In fact the displacement of the ICE is inferior with regards to a traditional vehicle, it works at a fixed point, and it can be acoustically isolated and allocated on the back end of the vehicle
- The vehicle can work, if necessary, in pure electric mode and access to specific regulated urban areas (such as galleries and city centres)

On the other hand, series hybrid vehicle present the following main disadvantages with respect to the other hybrid categories:

- The overall layout is complex.

- During long missions, the maximum power deliverable by the vehicle is not always available.
- The battery pack is heavy and expensive.

The three main unities of series vehicles are:

- the electric power generation group, composed by ICE and electrical machine
- the storage unit
- the traction unit represented by the powertrain

Among all these elements, power converters are present and play the role of interface between different units. Power converters have the purpose of convert the energy in different forms as well as control the flux of power. A stabilizer is also present between the source of electrical energy and the power converter. The stabilizer sets the minimum voltage value next to electrical component (generator, battery and electrical machine for traction) and a higher value for the circuit among power converters, in order to decrease the value of the current and consequently the cost of solid wires. In fact, for a given value of voltage, the cost raises directly proportional to the current.

The generation unit is generally sized such as it is able to deliver energy to the battery according to the mean power requested by the driving mission. The main reason lies in the fact that the ICE may as much as possible around its best condition in a stationary way. As consequence, the overall efficiency of the vehicle is enhanced and the fuel consumption is lowered.

The storage unit must possess the capabilities to supply higher power levels with respect to the mean one during the acceleration phases, and to store the energy coming from the braking phases. Their main features should be:

- high charging and discharging efficiencies
- high nominal specific power
- reduced self-discharge

The size of the battery depends, rather than from the mean power requested by the driving mission, by the maximum peak current value during the charging/discharging phases, and by the fact that it must preserve its discharging capacity. Battery capacity and battery life are inversely proportional parameters that are set according to economic and technical reasons. Practically, a reduced capacity implies a minor cost of the component, but on the other hand an enhanced capacity extends the battery life and so the maintenance cost is reduced.

An eventual power boost may be installed between the generator and the battery, mainly supercondensers or fly-wheels with electrical interface. It can enhance the capacity of the system to provide peak value of power during critical phases of the mission,

and also to regenerate the braking energy in a more efficient way. The main advantages of a vehicle that adopt this solution is:

- enhanced autonomy in pure electric modality
- higher performances, independently by the state of charge of the battery
- reduction of peaks of current values and consequent extension of battery life

The present chapter illustrates the concept of a novel implementation in the *optimization tool* whose peculiarities have been illustrated in chapter 3. The concept of a series HEV architecture has been derived from the *p2p4* hybrid architecture, whose functioning modes are described briefly in the following paragraph. In fact, figure 3.1 represent a *p2p4* HEV vehicle; by looking at its layout it is possible to imagine the functioning of a series HEV by disjointing the frontal powertrain (depicted in yellow) from the ICE. This operation is easily practicable by the control unit, being the frontal powertrain and the ICE separated by a mechanical clutch. For these reasons, in the present document the series HEV is also intended as *p2p4s*.

The *p2p4* architecture of figure 3.1 is hence a complex hybrid, because it both the functionality of a parallel hybrid and a series hybrid. Nevertheless, in the present study the implementation of the series layout is intended as stand-alone, assuming that the frontal powertrain always remains disengaged during the mission. Consequently, the totality of the power supplied by the internal combustion engine is absorbed by the frontal electric machine, that works as generator.

3.1 P2P4 layout

In the *p2p4* the internal combustion engine is mechanically coupled with the front electric machine EM1 by means of a torque coupling device. The front powertrain is composed by a gearbox and a final drive mounted on the frontal axle. A second electric machine is present, and it is connected with the rear powertrain.

The equations that describe of power of the internal combustion engine P_{ice} , frontal electric machine P_{em1} and rear electric machine P_{emr} are derived recalling the definition of sub-control variables α and ϕ , that represent the power subdivision between the front and rear powertrain and the power subdivision between the EM1 and the ICE respectively:

$$P_{ice} = (1 - \alpha) \cdot P_f \quad (3.1)$$

$$P_{em1} = \alpha \cdot P_f \quad (3.2)$$

$$P_{emr} = P_r \quad (3.3)$$

where P_f is the request of power supplied by the front powertrain and P_r is the request of power supplied by the rear powertrain.

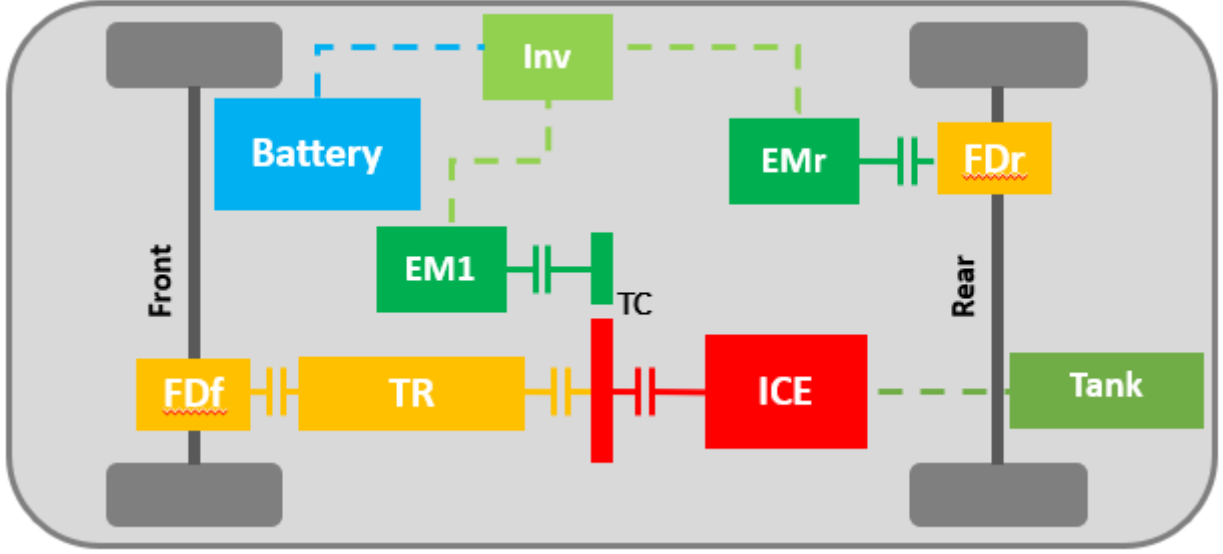
Figure 3.1. $P2P4$ layout representation

Table 3.1 illustrates all the possible powerflow modalities that are possible to obtain in a $p2p4$ architecture:

- PE: represents the *pure electric* mode, that can be enabled in three different ways. In the two cases, only a single electric machine is working, EM1 and EMr respectively. In the third case, both electric machine are providing power towards their dedicated powertrain.
- PT: represent the *pure thermal* mode, where only the internal combustion engine is switched on and supplies mechanical power through the front powertrain.
- PS: represents the *power split* mode, typical of parallel architectures, where the internal combustion engine is assisted by the electric motor in the traction phase. The power share is regulated by factor α by means of equations 3.1 and 3.2.
- BC: represent the *battery charging* mode. This configuration is obtained by disengaging the clutch of the front powertrain. In this way, the mechanical power supplied by the internal combustion engine flows into the electric machine that works as generator, converting that amount of power into electric energy. This particular powerflow is characterized by negative values of α . Another

3.2 Proposed model

The series hybrid architecture has been modelled according to the scheme of figure 3.2. It features the presence of an internal combustion engine, a fuel tank, two electric

Working mode	Components	α	ϕ
PE	EM1	1	0
	EMr	0	1
	EM1 + EMr	1	$0 < \phi < 1$
PT	ICE	0	0
PS	ICE + EM1	$0 < \alpha < 1$	0
	ICE + EMr	0	$0 < \phi < 1$
	ICE+EM1 + EMR	$0 < \alpha < 1$	$0 < \phi < 1$
BC	ICE + EM1	$-1 < \alpha < 0$	0

Table 3.1. $p2p4$ working modes

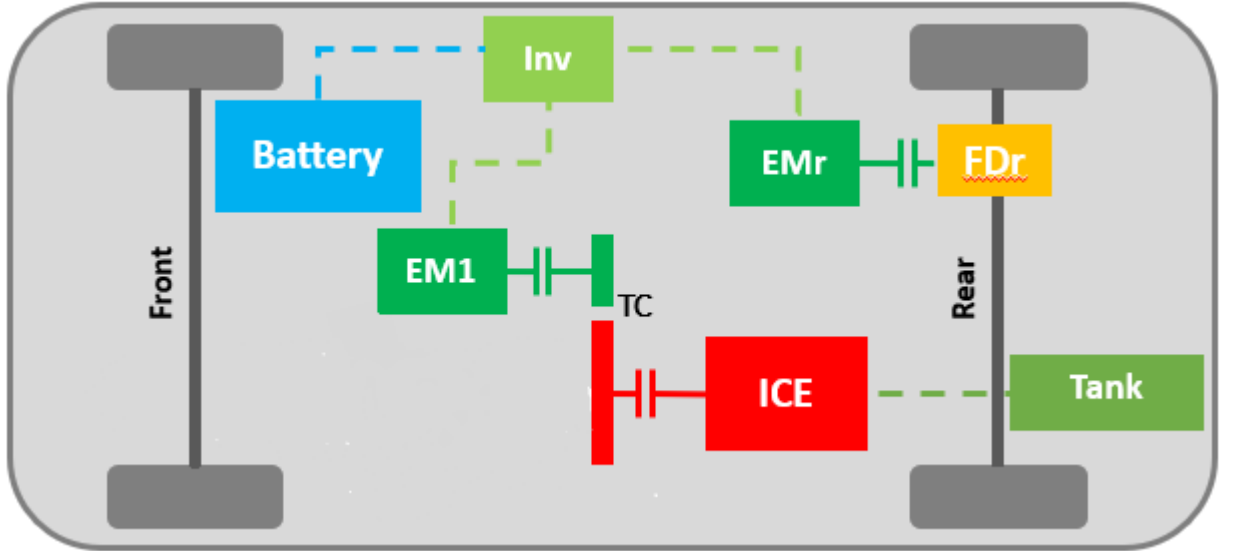


Figure 3.2. P2P4s layout representation

machines, a battery, power converts and a rear powertrain.

The totality of the power supplied by the vehicle comes from the rear power train. More in details, the rear axle is provided with a final drive that is mechanically coupled with the rear electric machine EMr. Through the final drive, the flux of power coming from the road is deviated towards the vehicle and absorbed by the electric machine during the braking phase. The opposite flux occurs in case of traction, where the electric machine EMr provides the power needed for the advance of the vehicle this meaning that the frontal powertrain is not employed in the proposed model.

By comparing figure 3.1 and 3.2 of the series and complex parallel p2p4 respectively,

it is possible to notice that the only difference is represented by the absence of the frontal powertrain, depicted in yellow in figure 3.1. The series traction configuration is in fact possible to obtain also in p2p4 architectures by mechanically disengaging the frontal drive with a clutch. In this case, the frontal powertrain would not transmit any flux of power to the frontal axle. As a consequence, its components, namely the transmission (also indicated as gearbox) and the final drive, would result disconnected from the rotating parts of the vehicle. In this case, being the shafts that connect the gearbox with the final drive motionless, the flux of power cannot flow from the generator unit towards the frontal axle. As consequence of these considerations, being the proposed series vehicle model derived from the complex p2p4 architecture, it can be also labelled as p2p4s. However, in the present study the p2p4 hybrid vehicle is not intended as a complex hybrid vehicle with both parallel and series functioning modes, even if it possesses the capabilities thanks to its configuration. The only working modes of p2p4 layout are in fact described in the previous chapter and they resolve into a parallel configuration only.

Thanks to the consideration listed below, it is possible to derive two fundamental characteristics of the model:

- the amount of split of requested power among frontal and rear axle is trivial in the p2p4s architecture
- the gear number is not a required parameter to describe the system

3.2.1 Evaluation of the requested power

Recalling that P_v the power requested by the vehicle estimated along the mission through the equation 2.22 and the approach illustrated in the previous chapter, the definition amount of power split among axles is:

$$P_{wh,f} = (1 - \phi) \cdot P_v = 0 \quad (3.4)$$

$$P_{wh,r} = \phi \cdot P_v = P_v \quad (3.5)$$

hence the sub-control variable ϕ , that describe the power flow in terms of ratio between the total power requested and the power at the rear axle, always assumes the value equal to 1 in the proposed model.

The rotational speed of the shaft of the rear electric machine is directly linked to the angular speed of the rear wheels by means of a rear final drive, i.e. a transmission ratio τ_r . It is possible to derive the angular speed of the rear electric machine:

$$\omega_{emrr} = \tau_r \cdot \omega_{wh,r} \quad (3.6)$$

and its rotating inertial power can be estimated as:

$$P_{emr,in} = I_{emr} \cdot \dot{\omega}_{emr} \cdot \omega_{emr} \quad (3.7)$$

Concluding, the totality of power requested for the advance of the vehicle is supplied by

the rear powertrain. The value of energy delivered by the rear powertrain $P_{req,r}$ embeds the contribution coming from the inertial rotation of the electric machine, described by equation 3.7, and the power at the street level P_v coming from 2.22

$$P_{req,r} = P_v + P_{emr,in} \quad (3.8)$$

3.2.2 Metamap

This section illustrates the method of the creation of the *metamap*, that is used for the selection of efficient points of the system. A similar approach can be found also in other studies [14] [15].

The electric power generation group is composed by the internal combustion engine (ICE) and the electric machine (EM1) depicted in figure 3.2 respectively by the red and the green boxes. They are connected by means of a torque coupling device. The objective of the generation group is to provide electrical power. This energy can be stored in the battery or directly delivered to the rear electric machine for traction purpose, depending on the control employed by the vehicle and the strategy adopted. In fact, the values and modalities of generation of mechanical power by means the ICE and transformation into electrical by EM1 represent the main characteristics of a series hybrid vehicle. The lack of a gearbox and constricted degrees of freedom in the distribution of power among components are important disadvantages of a series architectures; on the other hand the coupled system of the internal combustion engine and the electric generator are mechanically disjointed from the powertrains, permitting consequently a total control on the working points of the unit. More in details, by referring to a p2p4 architecture (figure 3.1) the internal combustion engine rotational speed is unequivocally derived as consequence of the value of rotating speed of the wheels on the frontal axle. The presence of the gearbox is fundamental in order to mitigate this constriction by adding extra degrees of freedom with the use of gears. Still, given the linear speed of the vehicle, the possible values of rotational speed that the internal combustion engine can assume are derived and discrete. The same considerations hold for the rotational speed of the frontal electric machine EM1. In case of a series hybrid architecture, the control over the engine rotational speed and combined torque, i.e. the working point on the characteristic map, is completely unrestricted and continuous. The criteria of the choice of the working points of the generation unit, whose controls and strategies are described in details in the following sections of the present chapter, rely on the best efficiency possible of both internal combustion engine and the electric machine. Hence, the proposed model introduces the idea of combined efficiency, or global efficiency. Let us assume to pick a working point on the internal combustion engine map, where efficiencies of conversion of energy from thermal into mechanical are reported. The working point contains informations about the rotational speed of the motor ω_{ice} , the value of torque T_{ice} , the mechanical power provided P_{ice} (obtained by the product of speed and torque) and the efficiency of the point itself η_{ice} . The corresponding working point on the electric machine EM1 is directly a consequence of the one of the internal combustion engine. In fact, by means of the torque coupling device, it is possible to

write:

$$\omega_{em1} = \tau \cdot \omega_{ice} \quad (3.9)$$

$$T_{em1} = -\frac{T_{ice}}{\tau} \quad (3.10)$$

where τ is the transmission ratio of the torque coupling device. The couple of values ω_{em1} and T_{em1} uniquely identify the working point on the map of the electric machine, thus an efficiency value $\eta_{em1}(\omega_{em1}, T_{em1})$. The minus sign present in equation 3.10 has been introduced, meaning that the power of the electric machine is absorbed, hence characterized by a negative value. It is worth noticing that in the series configuration the electric machine EM1 always works in the part of the map with negative torque, i.e. as generator. This procedure holds for any working point chosen on the ICE map, projected on the generator map of EM1 through the transformation equations listed above. Therefore it is possible to consider the separated working points on the ICE and EM1 as an unique working point. Its efficiency η_{global} is obtained as the product of the individual working points, expressed as:

$$\eta_{global} = \eta_{ice}(\omega_{ice}, T_{ice}) \cdot \eta_{em1}(\omega_{em1}, T_{em1}) \quad (3.11)$$

As consequence of the consideration listed above, a new map is introduced, referred as *metamap*, in which the map of the ICE is projected, through axis transformation, onto the generator map of EM1. The internal points of the metamap represent the combined global efficiency of the working point of the system (figure 3.2.2). The metamap is involved in the definition of working points along the mission of the vehicle, and its utilization depends on the strategy adopted. More in details, the metamap is substantially employed in the following occasions:

- when a given level of power is required
- when a given level of power and rotational speed of components are required

In the first case, the requested level of power P is compared with the maximum power deliverable by the internal combustion engine and the electric machine. If the value of P represents a feasible value for the generating unit, namely it is contained in the domain of the metamap, the locus of points constituted by all the couples of rotational speeds and torques that supply that specific level of power is individuated on the metamap. Among these values, the selected working point is the one that features the maximum value of global efficiency.

In the second case, the metamap simply provides the value of global efficiency associated to the requested level of power P and rotational speed ω .

3.3 Control strategies

An effective control strategy of a serial stand-alone hybrid vehicle considers all the possible configuration of operating modes, namely the different modalities of traction

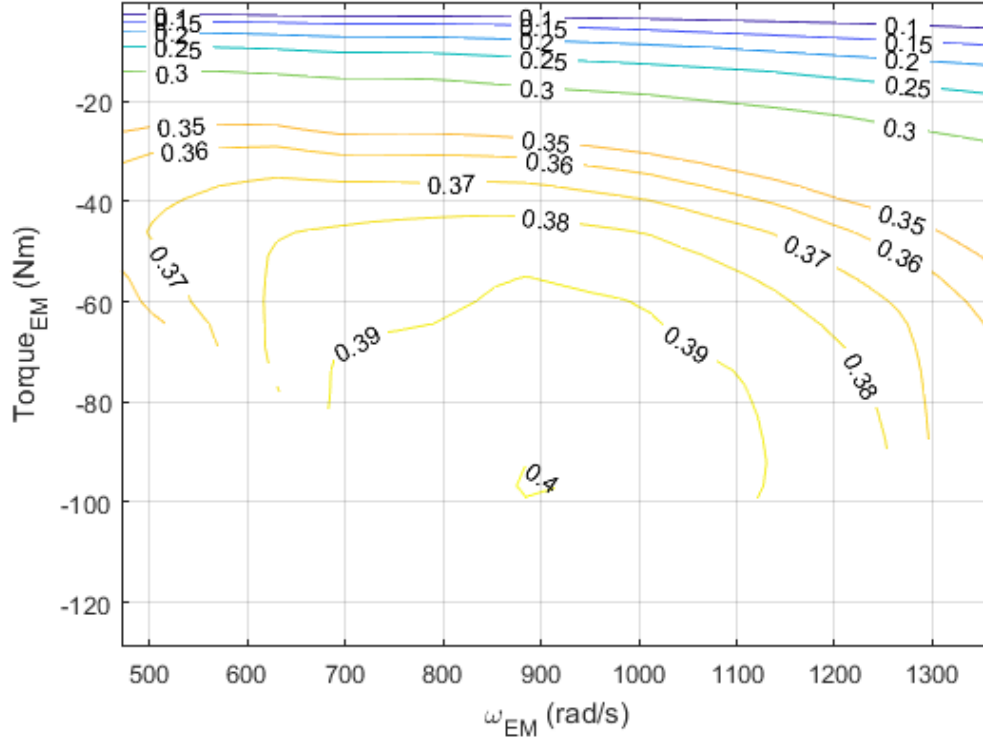


Figure 3.3. Representation of the metamap

that can occur during the driving mission. A qualitative description of the possible operating modes that are considered in the present study is herein presented:

- *pure electric* : in the pure electric mode (PE) the internal combustion engine is switched off, hence no electrical power is delivered by the generator. In case of traction phase, the request of power is totally supplied by the battery. As a consequence, the state of charge of the battery during pure electric traction operation necessarily decreases. On the other hand, this operating mode is also adopted whenever the vehicle brakes across the driving mission. In this case, regenerating brake phenomenon occurs and the state of charge of the battery increases.
- *charge sustaining* : the charge sustaining mode (CS) is a particular operating mode typical of series HEV in which the power requested by the rear powertrain for the advancement is exactly provided by the generator EM1 through conversion of mechanical energy coming from the internal combustion engine. Consequently, during charge sustaining operations no flux of energy is involved around the battery and the value of SOC remains constant over time.

- *battery charging/depleting* : an extra degree of freedom in the management of power is present in series vehicles and it is represented by the battery charging/depleting operation. This specific operating mode has been designed in order to have the possibility to deal with a fixed amount of power with the generating unit, independently from the value of requested power by the rear powertrain. In this case, the internal combustion engine is assigned to work around a given fixed point, hence at constant angular speed and torque, or different groups of points. As a consequence, the amount of power that the EM1 generator provides is constant and not related to the request that comes from the powertrain. The internal combustion engine and the generator that work at fixed point can both function in battery charging and battery depleting mode. More in details, in case of higher power provided by the generator with respect to the requested one, the extra amount of power creates a surplus of energy that is stored in the battery. Therefore, the value of SOC raises and the vehicle is working in battery charging mode. On the other hand, when the power provided by the generator is lower with respect to the requested one, the battery covers the net of energy needed for the advancement of the vehicle. Consequently, in this case the vehicle is working in battery depleting mode and the SOC level decreases.

It is important to remark that the operating strategies described above are all essential for the realization of a series stand-alone architecture. Each operating mode can in fact be seen as a "degree of freedom" of the vehicle, that makes it capable to complete the given driving mission within the given boundary conditions. More in details, the SOC level can be correctly managed by the optimizer thanks the possibility to range over pure electric, charge sustaining and battery charging/depleting modes. This aspect is fundamental being the driving mission SOC constrained, namely the SOC must always be contained in a range called *SOC window* represented by the values of SOC_{max} and SOC_{min} ; moreover the initial condition of the state of charge SOC_0 must be equal to the state of charge at the last temporal stage of the mission SOC_{end} .

Two possible approaches of implementation and control are proposed in the next part of this chapter. In the first approach, the values of intermediate variables (namely physical quantities associated to the vehicle components) are derived by doing considerations on the behaviour of components in the different operating modes that feature the serial stand-alone architecture. The second approach introduces the concept of the utilization of rotational speeds of the internal combustion engine as sub control variables. For these reasons the first control methodology is called *working-modes control* and the second is labelled as *speeds control*.

The two methods have the following aspects in common:

- the gear number GN is no more representative of an effective degree of freedom of the system, contrary to what happens in p2p4 parallel architectures. In series architecture in fact the gearbox is disengaged from the frontal transmission, being the frontal powertrain itself not involved in the traction system. Therefore, the gear number is no more considered as a control variable of the vehicle that constitutes the multiplicity of working modes.

- the flux of power only flows in the rear powertrain, being the rear electric machine EMr addressed for the distribution of mechanical power to the axle for traction. Therefore, the sub control variable ϕ that describes the power split among the two axes is always equal to one.

3.3.1 Working-modes control

In the *working-modes* control approach the only control variable is the powerflow, which defines the power split among powertrain components. The intermediate variables are derived according to the specific working mode and the requested power at the rear powertrain.

Pure electric

During pure electric operations, adopted during traction and braking phases, the internal combustion engine and the electric generator are switched off. The rotational speed assigned to pure electric working mode are zero for both the two components. Consequently, also the power provided by the internal combustion engine and the electric generator is null. The value of the sub-control variable α that describes the powerflow is set equal to zero.

Charge sustaining

In charge sustaining operations (CS) the vehicle power demand is directly satisfied by the internal combustion engine, that exactly provides the requested level of energy needed for the advancement across the interval of time. This particular powerflow is identified by the parameter α associating the conventional value of minus infinite. The equation that links the power provided by the internal combustion engine along the mission and the rear powertrain demand is the following:

$$P_{ice} = P_{req,r} = P_v + P_{in,emr} \quad (3.12)$$

recalling that in the configuration matrix approach each physical quantity involved in the description of the system is a column of the configuration matrix related to that specific physical quantity, here represented by the terms that compare in the equations. Moreover, each column represents a working mode given by the combination of all the different control variables. In the equation 3.12 the term P_v represent the power requested at the street level and $P_{in,emr}$ is the inertia of the rear electric machine. These two values are unequivocally derived from the input variables of vehicle velocity over time and street slope; the energy transformation losses from mechanical to electrical and vice versa are neglected. The power associated to the electric generator P_{em1} is equal in modulus and opposite in sign to the power provided by the internal combustion engine P_{ice} .

The values of speed and torque of internal combustion engine and electric machine adopted along the driving mission, i.e. the working points of the system, are chosen

according to the global efficiencies of the coupled components that reported in the Metamap. More in details, each power level of the internal combustion engine and electric generator (that are associated to the various time intervals) is identified on the Metamap by means of a hyperbole. Each hyperbole represents the locus of points that are capable to provide that exact amount of power, obtained combining different values of rotational speed and torque, namely different working points. Finally, the working point of a specific interval of the mission is determined by selecting the most efficient working point among all the possible ones that lie in the given hyperbole. The ensemble of all the working points obtained for the charge sustaining operation are represented in the figure 3.3.1; the points that coincides with the origin of the map are the ones that represent the braking phases, during which the internal combustion engine is switched off as well as the electric generator.

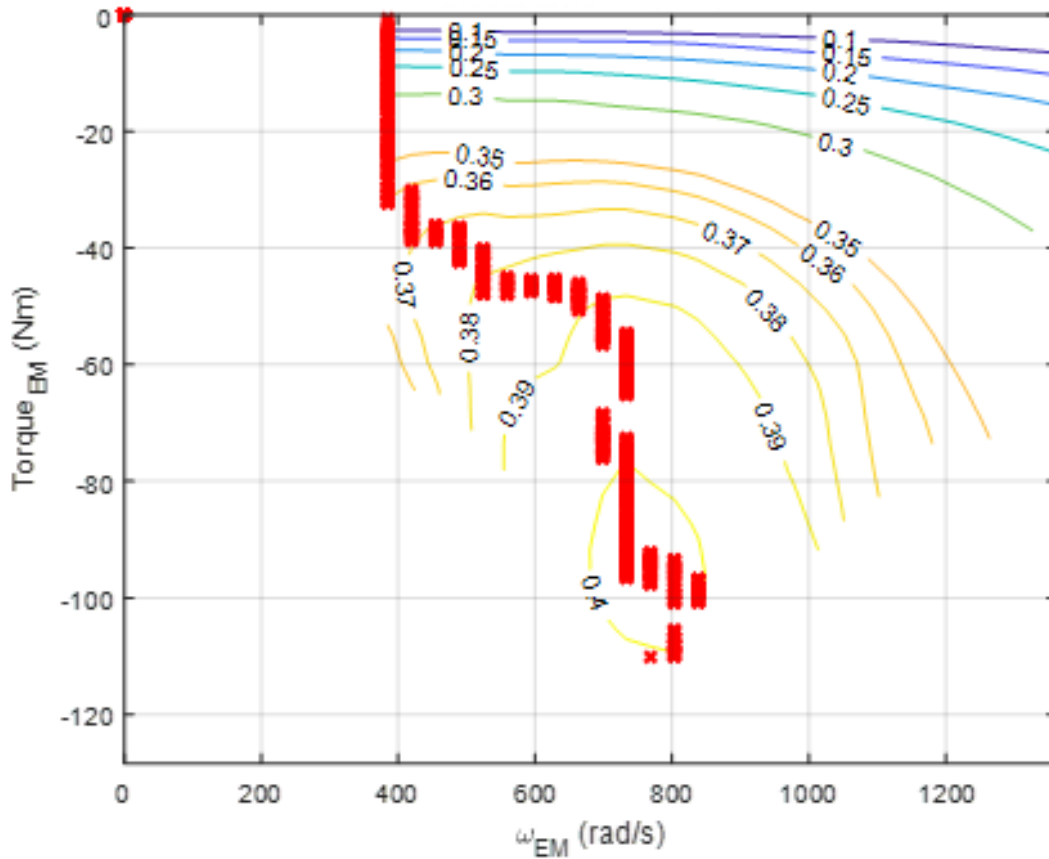


Figure 3.4. Working points in CS operation represented in the Metamap

Battery charging/depleting

The battery charging/depleting operating mode has been designed in order to enhance the flexibility of the vehicle, under the aspect of management of power fluxes and SOC

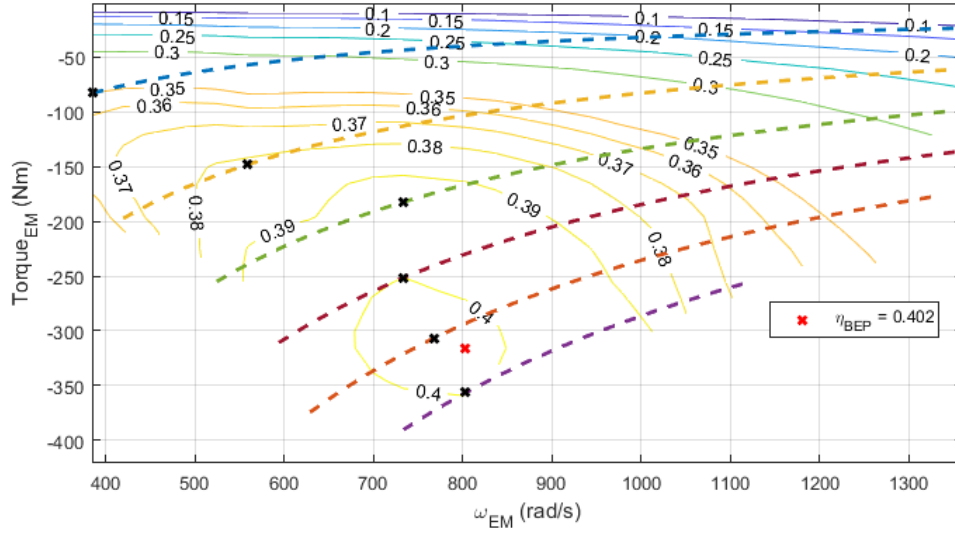


Figure 3.5. Representation of battery charging/depleting working points on the metemap

level. More in details, in this case the value of the requested power that comes from the rear powertrain is not considered, and the internal combustion engine works around a fixed point providing a constant amount of energy to be delivered towards the battery. This operating mode permits a high flexibility in the choice of working points of the generating group and in the amount of power consequently delivered. The criteria in the definition of the internal combustion engine rotating speed and torque are mainly two:

- the working points must lie around efficient regions of the Metamap
- the number of power levels must be sufficiently high to cover the request of energy that comes from different moments of the driving mission

An example of battery charging/depleting design is represented by the figure 3.3.1, showing the Metamap and the set of working points in battery charging/depleting mode. More in details, the red cross represents the best efficiency point (BEP), while the dashed hyperboles represent different power levels. In this example, six power levels have been considered, distributed in order to cover in an equispaced manner the totality of the area of the Metamap. Moreover, the working points on each power level, indicated by the black crosses, are chosen with the identical procedure adopted in the charge sustaining case. On the other hand, in battery charging/depleting operating mode the columns of the configuration matrices are compiled with the same values from the beginning to the end of the driving mission. The equispaced distribution of power levels ranges from the minimum to the maximum value of power that the coupled system ICE-EM1 can supply. This approach allows the optimizer for a total

flexibility in the management of the SOC level, regardless from the instantaneous value of required power.

3.3.2 Speeds control

The *working mode control* approach described in the previous section is based on the control of the operating mode of the vehicle. In that case, the optimizer performs the optimal choice by selecting at each stage different operating conditions among pure electric, charge sustaining and battery charging/depleting. The values of intermediate variables, namely all the physical quantities related to internal combustion engine, electric generator and battery, are consequently assigned to each component according to the working mode. In that case, the parameter that describes the control of the vehicle is the sub-control variable α , namely the powerflow. A different approach is proposed in the present section, where the control of the vehicle is directly executed on the rotating speed of the internal combustion engine. In fact, the principal characteristic of series HEVs layout is represented by the internal combustion engine that is mechanically disengaged from the transmission, allowing for a complete regulation on rotating speed, torque and power delivered. Moreover, this approach allows for a better description of the system, allowing to evaluate the inertial terms of internal combustion engine and electric generator.

The *speed control* approach regulates the vehicle according to the choice of the rotating speed of the internal combustion engine; the new sub-control variable that describes the problem is ω_{ICE} , and it represents the rotating speed of the internal combustion engine expressed in radians per second. It is recalled that the time domain of the system is divided in N_{in} number of intervals. Each time interval, that represents the singular temporal stage of the driving mission, can be described by means of control variables, input variables and intermediate variables. For example, let us consider the generic physical variable v ; each time interval i is described by the values of v assumed at the rightmost node of the interval $v_r(i)$ and at the leftmost node of interval $V_l(i)$. The objective of the *speed control* approach is to give a complete description of the system, by considering all the possible variation of velocities of the internal combustion engine that can occur in a time interval, by the means of $\omega_{ICE,r}$ and $\omega_{ICE,l}$. This considerations are necessary in order to exploit the *deterministic dynamic programming optimizer* (DDPO), that requires a deterministic knowledge of the system, in terms of temporal evolution and possible combination among states. The set of N_ω discrete rotating speeds of the internal combustion engine can be defined as:

$$S_\omega = \{\omega_1, \dots, \omega_N\} \quad (3.13)$$

Consequently, the number of speed configurations $N_{conf,\omega}$, defined as the number of possible speed variations between the right end and the left end along a single interval is:

$$N_{conf,\omega} = N_\omega^2 \quad (3.14)$$

Therefore, the configuration matrices that describe the physical quantities involved in the system have dimensions:

$$M_v \in \mathbb{R}^{N_{in} \times N_{conf}} \quad (3.15)$$

where v is the generic variable, N_{in} is the number of row equal to the number of time interval and N_{conf} is the number of columns obtained as:

$$N_{conf} = N_{conf,\omega}^2 \times N_{ES} \quad (3.16)$$

For example, let us consider the simple case in which the internal combustion engine can be regulated over three rotating speeds, namely ω_1 , ω_2 and ω_3 . The number of speed configurations is obtained as $N_{conf,\omega} = N_{\omega}^2 = 9$; the table 3.3.2 shows the combination of rotating speeds as a function of the configuration index:

Configuration Index	$\omega_{ICE,r}$	$\omega_{ICE,l}$
1	ω_1	ω_1
2	ω_1	ω_2
3	ω_1	ω_3
4	ω_2	ω_1
5	ω_2	ω_2
6	ω_2	ω_3
7	ω_3	ω_1
8	ω_3	ω_2
9	ω_3	ω_3

Table 3.2. Representation of speed variations combinations on a single time interval

The value of rotating speeds of electric generator EM1 are consequently derived multiplying the rotating speeds of the internal combustion engine by the transmission ratio of the torque coupling device τ_{au} . Finally, it is possible to evaluate the inertial power of the internal combustion engine and the electric generator thanks to the formula 3.17, for each combination of speed variation:

$$P_{in} = I \cdot \dot{\omega} \cdot \omega \quad (3.17)$$

where I is the moment of inertia and $\dot{\omega}$ is the acceleration.

Chapter 4

Results

The behaviour of the proposed model of a series hybrid vehicle has been investigated in the *optimization tool* environment described in chapter 2. More in details, the interest of the present study has been directed towards the implementation of an effective control strategy of the vehicle, able to achieve the accomplishment of a given driving mission. This chapter illustrates the results obtained from the implementation of the *working-modes control* and the *speeds control* strategies, previously described in paragraphs 3.3.1 and 3.3.2 respectively.

The vehicle considered in the present study belongs to the *heavy-duty* typology, classified according to the Directive 2007/46/EC of the European Parliament [16], that comprehends trucks, buses, and coaches. The parameters of the above-mentioned vehicle that have been implemented are summarized in table 4.1.

Parameter	Description	Value	Unit of Measure
M_{curb}	Vehicle Curb Weight	4200	[kg]
M_{fl}	Full-load Weight	7500	[kg]
R_{wheel}	Wheel Radius	0,37	[m]
J_{wheel}	Wheel Inertal Modulus	3	[kgm ²]
η_{wheel}	Wheel Efficiency	0,9	[-]
n_{wheel}	Number of Wheels	4	[-]
C_x	Aerodynamic Resistance Coefficient	0,703	[-]
A_f	Frontal Section	6,5	[m ²]
R_{roll}	Rolling Resistance Coefficient	0,0879	[N/kg]

Table 4.1. Heavy-duty Vehicle Parameters.

The reference driving mission that has been considered is the World Harmonized Vehicle Cycle (WHVC). This cycle covers the typical driving condition of a heavy-duty vehicle in EU, Japan, United States and Australia. It is divided in three segments,

representing urban, rural and motorway driving, for an overall duration of 1800 seconds. Figure 4 illustrates the profile of velocity with respect to time and provides a detailed description of the three parts of the mission:

- the first segment lasts 900 seconds and represents the urban section. It is characterized by frequent starts, stops and idling; the peak velocity is 66 km/h and the average velocity is 21,3 km/h.
- the following segment lasts 481 and represent the rural driving section. The peak velocity is 76 km/h and the average velocity is 43,6 km/h.
- the last segment represents highway driving condition with peak velocity of 88 km/h and average velocity of 76,7 km/h. This part lasts 419 seconds.

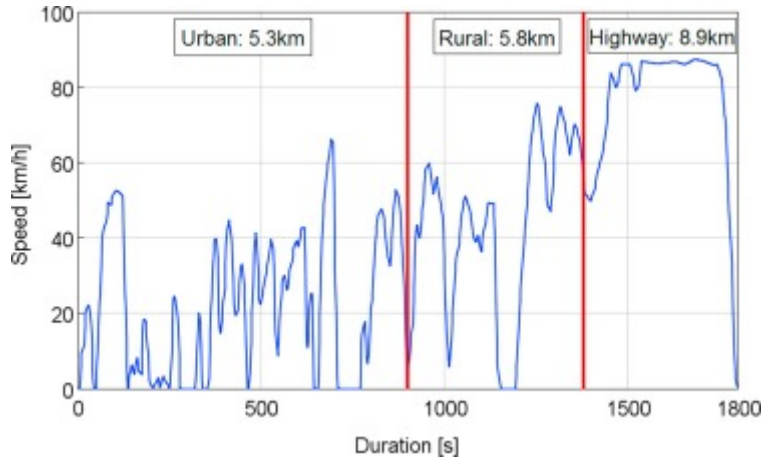


Figure 4.1. WHVC cycle.

4.1 Comparison between working-modes control and speeds control

The two different approaches *working-modes control* and *speeds control* have been compared by means of various simulations on the same vehicle architecture. The size of the components and the transmission ratios are reported in table 4.2, where the *PE ratio* is a parameter that accounts for the battery size and is defined as the ratio between the sum of the peak power of electrical machines and the battery energy storage capacity, *GB ratio* represents the transmission ratio of the torque coupling device and *FDr ratio* is the transmission ratio of the speed coupling device of the rear powertrain.

The output parameter that have been considered as indicator of precision and quality of the control strategy is the quantity of CO₂ emitted along the driving cycle. In fact, the value of CO₂ emissions is directly derived from the optimization procedure

Parameter	Unit of Measure	Value
Engine Displacement	[dm^3]	3,6
PE Ratio	[-]	12
EM1 Size	[kW]	120
EMr Size	[kW]	130
GB Ratio	[-]	6
FDr Ratio	[-]	19

Table 4.2. Series layout adopted for the comparison between different control strategies.

performed by the dynamic programming over the objective function, namely the fuel consumption. Moreover, an immediate comparison between different architectures and control strategies can be obtained simply evaluating the value of total or specific CO₂ emission along the driving cycle, without considering its temporal evolution.

The choice of the control parameters has been made according to the specific control strategy. More in details, for the *working-modes* approach it is needed to provide the number of modes that characterize the simulation. Moreover, each working can be addressed to a specific powerflow, namely pure electric, charge sustaining and battery charging/depleting. On the other hand, the *speeds* approach must be provided with the number of speeds that the internal combustion engine can assume. Also in this case, each speed is addressed to a specific working condition, that can be pure electric, charge sustaining or fixed point for battery charging/depleting operations. Hence, for both the control strategies it is possible to identify a number of *degrees of freedom*, namely the different configurations that the vehicle can assume during the driving mission, that is represented by the number of working modes for the first approach and the number of speeds of the internal combustion engine for the second approach. This number has been taken into account for a proper comparison between the *working-modes control* and *speeds control*.

Figure 4.1 illustrates the results obtained in terms of CO₂ emissions as function of degrees of freedom of the vehicle, represented by the number of configurations and the number of speeds of the internal combustion engine for *working-modes control* and *speeds control* approach respectively. It is possible to notice that the emissions obtained adopting the *speeds control* are considerably higher with respect to the ones obtained with the *working-modes control*, by 14% on average. This expected result is due to the fact that the *speeds control* approach considers and evaluates the energy required to overcome the inertial resistances to speed variations of the internal combustion engine and the electric generator. On the other hand, in *working-modes control* this aspect is neglected, hence a variation of the working point does not causes any extra energy to be provided by the internal combustion engine, with the consequent emission of pollutants.

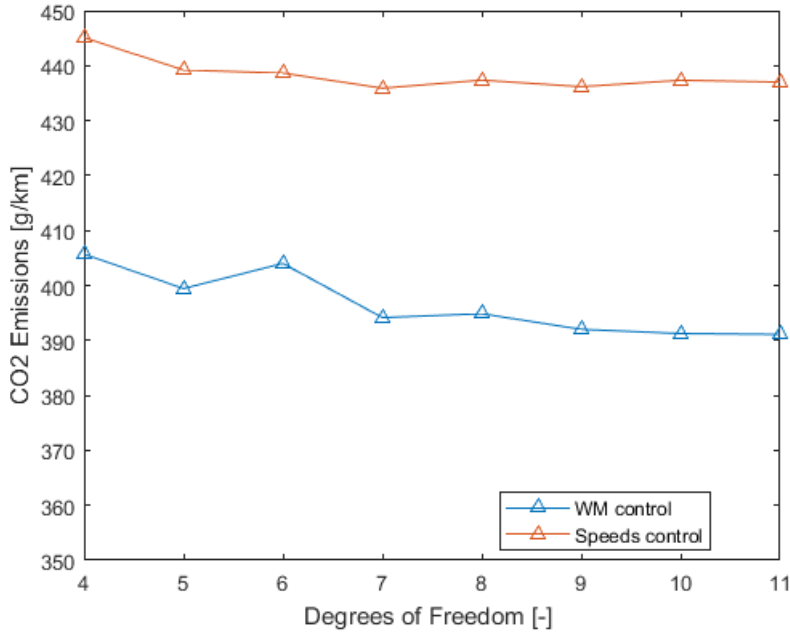


Figure 4.2. CO₂ emissions vs Degrees of freedom of the vehicle.

4.1.1 Considerations on computational time

Figure 4.1.1 illustrated the computational time of simulations as a function of the degrees of freedom of the vehicle. It can be noted that the time required to carry *speeds control* simulations, depicted in red, is one order of magnitude superior with respect to *working-modes control* simulation. This parameter mainly depends on the size of the configuration matrices that are provided to the optimizer. In fact, the number of configurations in the *speeds control* case it is proportional to the square of the number of speeds that the internal combustion engine can assume, while in the *working-modes control* case it is equal to the number of configurations of the vehicle.

4.2 Power profiles

The power profiles of the main components along the driving mission are herein investigated, obtained with *speeds control* approach simulations.

Figure 4.2 illustrates a particular segment of the driving mission where the vehicle traction is obtained in battery charging mode. It can be observed that the profiles of the mechanical power provided by the internal combustion engine and the electric power generated by the electric machine are flat, as a consequence of the fact that they are working at fixed point. On the contrary, the profile of mechanical power provided

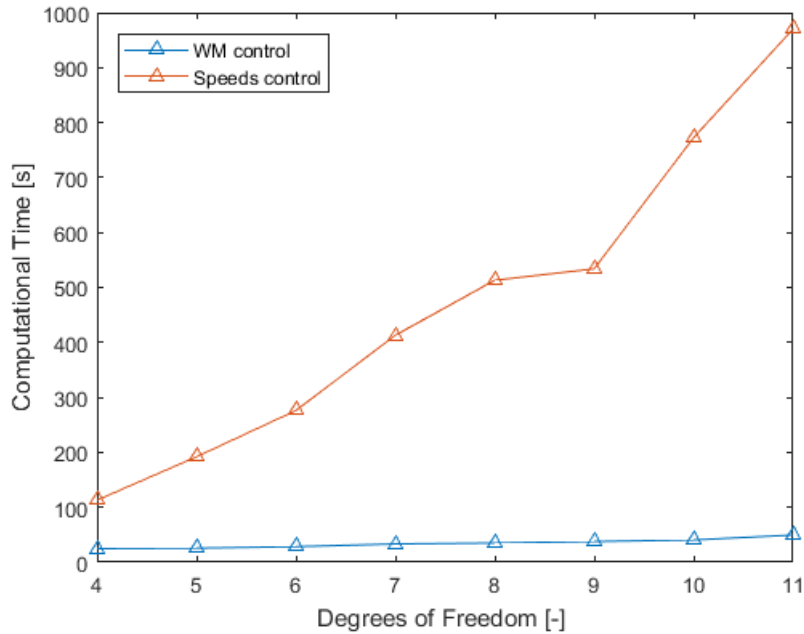


Figure 4.3. CO₂ emissions vs Degrees of freedom of the vehicle.

by the electric rear motor follows the trend of requested power of the vehicle at the street level.

On the other hand, figure 4.2 illustrates a portion of the driving mission where the vehicle is controlled in charge sustaining mode. In this case, all the power profiles of the component under investigation follow the trend of the requested power of the vehicle at the street level.

From both figures 4.2 and 4.2 it can be noted that the value of power from the road level to the innermost component of the vehicle, represented by the internal combustion engine, increases. This fact is due to the various losses that are present along the power flow distribution, that are represented by the conversions of energy between mechanical and electrical form, the conversions performed by the inverters and the inertial power possessed by the rotating components. More in details, in charge sustaining mode the mechanical power provided by the internal combustion engine is 40% higher with respect to the effective power exploited for traction. Finally, during battery charging operations the difference between the electrical power generated by the electric machine is 5,5% lower with respect to the mechanical absorbed power.

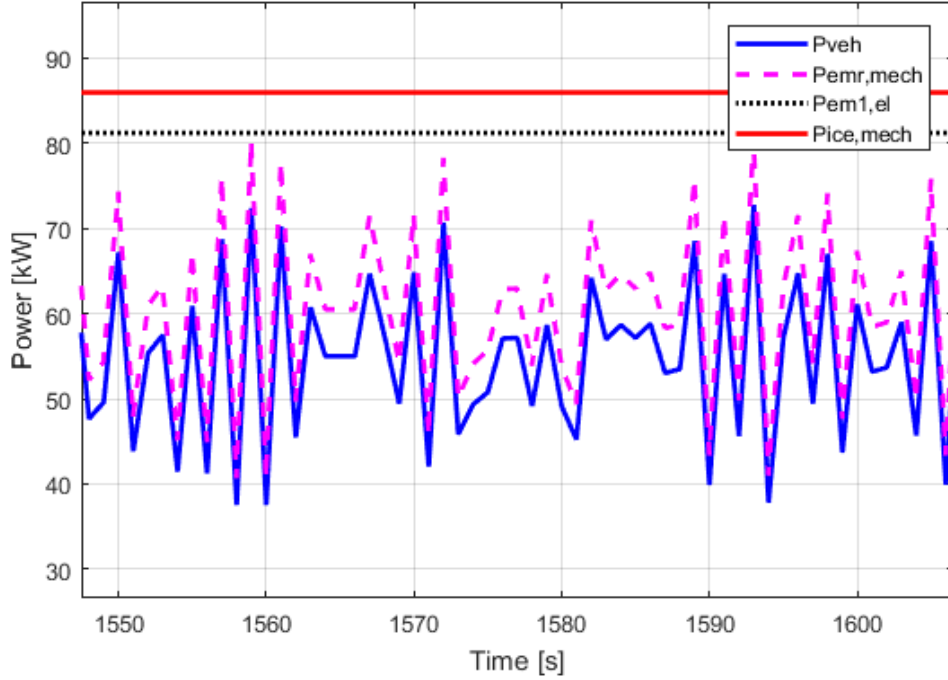


Figure 4.4. Detail of the diving mission performed in battery charging mode.

4.3 State of charge and powerflow profiles

Figure 4.3 reports the the results of a simulation performed with the *speeds control* strategy, including six possible rotating speeds of the internal combustion engine. Labels PE, BC/D and CS refers to the working modes that have been implemented with the control strategy, respectively pure electric, battery charging/depleting and charge sustaining. The initial value of the state of charge is imposed to 0,6 as well as the final value. The state of charge along the mission is constrained in a window between 0,4 and 0,8.

It is possible to observe that battery charging/depleting operations are widely selected by the optimizer, on an overall percentage of 31%. More in details, this powerflow is continuously exploited to recharge the battery at the end of the cycle where the vehicle enters in the most stressed segment, represented by the highway.

On the other hand, the first two segments of the cycle, namely the urban and rural parts, are performed with an even subdivision among the possible working modes, but with a discontinuous trend. The reason behind frequent shifts between them can be explained considering the nature of the WHVC cycle, that features many stops and demanding accelerations. For this reason, the optimizer chooses the most convenient working mode at each time step.

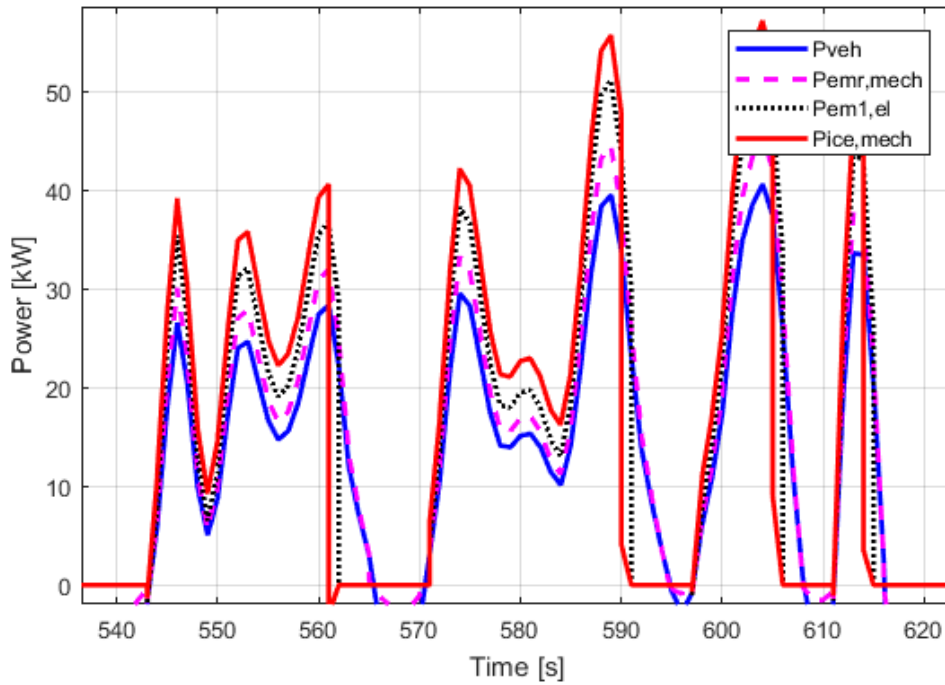


Figure 4.5. Detail of the diving mission performed in charge sustaining mode.

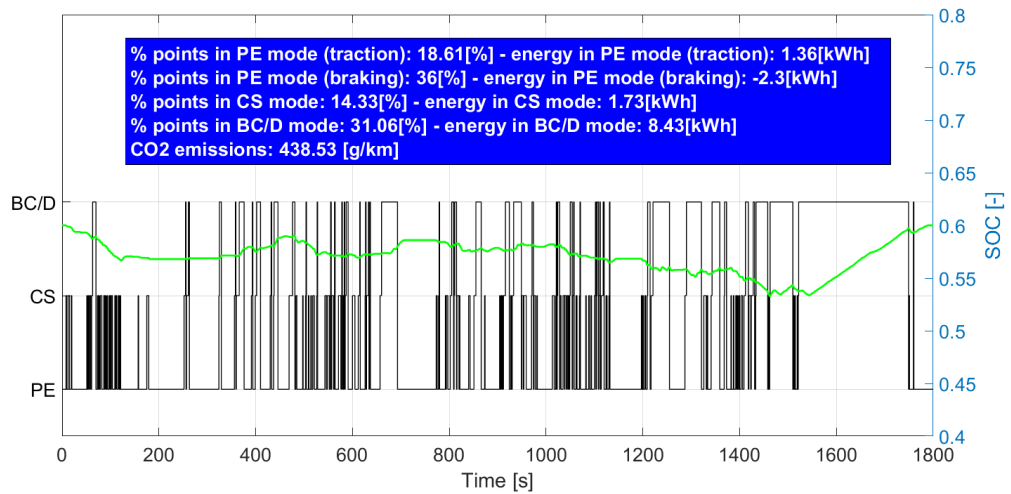


Figure 4.6. Optimal SOC and powerflow profiles on the driving mission

Chapter 5

Conclusions

In the present work a series hybrid vehicle architecture has been effectively implemented on the *optimization tool* developed in [1], through which it is possible to study the behaviour of hybrid vehicles and to optimize the control strategy over a selected driving mission. The proposed architecture is characterized by the following working modes, that are *pure electric*, *charge sustaining* and *battery charging/depleting*.

Two different control strategies have been proposed, namely the *working-modes control* and *speeds control*. In the first approach the only control variable is the powerflow, which defines the power split among the powertrain components. In the second approach the internal combustion engine speed is introduced as a new control variable. This allows to enforce its continuity over time, correctly assessing the inertial power of the engine and the electric generator's rotating masses.

In the results the two strategies are compared by running the dynamic programming algorithm for a *heavy-duty* vehicle over the WHVC cycle. The *working-modes control* strategy has shown far too low CO₂ emissions with respect to the *speeds control* strategy. This shows that neglecting the inertia of internal combustion engine and electric generator leads to unacceptable bias in the results.

Finally, the *optimization tool* permits to easily compare a large number of vehicle architectures, allowing to identify the optimal powertrain components sizing.

Bibliography

- [1] M. Venditti, "Innovative Models and Algorithms for the Optimization of Layout and Control Strategy of Complex Diesel HEVs", no. May, 2015.
- [2] European Commission, https://ec.europa.eu/growth/sectors/automotive/environment-protection/emissions_en [Online; accessed 03-April-2019]
- [3] E. D. Tate, O. Harpster, and Peter J. Savagian. "The electrification of the automobile: from conventional hybrid, to plug-in hybrids, to extended-range electric vehicles", SAE international journal of passenger cars-electronic and electrical systems 1.2008-01-0458 (2008): 156-166.
- [4] European Commission, "Results of the review of the Community Strategy to reduce CO2 emissions from passenger cars and light commercial vehicles," Commun. from Commission to Counc. Eur. Parlam., no. May, 2013.
- [5] A. Al-Samari, "Study of emissions and fuel economy for parallel hybrid versus conventional vehicles on real world and standard driving cycles," Alexandria Eng. J., vol. 56, no. 4, pp. 721–726, 2017.
- [6] Kamil Çagatay Bayindir, Mehmet Ali Gözükuçük, and Ahmet Teke, "A comprehensive overview of hybrid electric vehicle: Powertrain configurations, powertrain control techniques and electronic control units.", Energy Conversion and Management, 52(2):1305–1313, 2011.
- [7] W. Enang and C. Bannister, "Modelling and control of hybrid electric vehicles (A comprehensive review)," Renew. Sustain. Energy Rev., vol. 74, no. December 2016, pp. 1210–1239, 2017.
- [8] M. Awadallah, P. Tawadros, P. Walker, N. Zhang, "Comparative fuel economy, cost and emissions analysis of a novel mild hybrid and conventional vehicles." Proceedings of the Institution of Mechanical Engineers, Part D: Journal of Automobile Engineering, 232(13), 1846–1862.
- [9] Tate, E., Harpster, M., and Savagian, P., "The Electrification of the Automobile: From Conventional Hybrid, to Plug-in Hybrids, to Extended-Range Electric Vehicles," SAE Int. J. Passeng. Cars - Electron. Electr. Syst. 1(1):156-166, 2009.
- [10] G. Pede, E. Rossi, R. Vellone, "Esperienze di controllo e studi di ottimizzazione energetica per un veicolo ibrido serie," 2002.
- [11] X. Wang, H. He, F. Sun, and J. Zhang, "Application study on the dynamic programming algorithm for energy management of plug-in hybrid electric vehicles," Energies, vol. 8, no. 4, pp. 3225–3244, 2015.
- [12] B. C. Chen, Y. Y. Wu, and H. C. Tsai, "Design and analysis of power management

- strategy for range extended electric vehicle using dynamic programming,” *Applied Energy*, vol. 113, pp. 1764–1774, 2014.
- [13] Richard Bellman and Robert E Kalaba. *Dynamic programming and modern control theory*. Academic Press New York, 1965.
- [14] A. Solouk, M. Shahbakhti, M. Mahjoub, "Energy management and control of a hybrid electric vehicle with an integrated low temperature combustion (LTC) engine", *Proc. ASME Dyn. Syst. Control Conf.*, pp. V002T20A005, 2014.
- [15] Fan, J.; Zhang, J.; Shen, T. Map-Based Power-Split Strategy Design with Predictive Performance Optimization for Parallel Hybrid Electric Vehicles. *Energies* 2015, 8, 9946–9968.
- [16] EUR-lex <https://eur-lex.europa.eu/legal-content/EN/TXT/?uri=CELEX:32007L0046> [Online; accessed 03-April-2019]